PORT OTAGO MAINTENANCE DREDGING DISPOSAL STUDIES

Simulations of dredge disposal plumes and associated deposition at the proposed new Heyward Point Disposal Ground

Prepared for Port Otago Ltd

PO Box 441, New Plymouth, New Zealand
T: 64-6-7585035 E: enquiries@metocean.co.nz

MetOcean Solutions Ltd: P0140-06

July 2015

Report status

Version	Date	Status	Approved by
RevA	07/07/2015	Initial draft for internal review	Weppe
RevB	09/07/2015	Draft for client review	McComb
RevC	15/07/2015	Updated draft for client review	Weppe
RevD	01/08/2015	Updated draft	Weppe

It is the responsibility of the reader to verify the currency of the version number of this report.

TABLE OF CONTENTS

LIST OF FIGURES

1. INTRODUCTION

Dredging has been carried out in the Otago Harbour since the 1860s, with disposal of dredged material to sea occurring since at least 1882. Initially all dredged material was placed at the Heyward Point site, with Aramoana first being used in 1985 and Shelly Beach in 1987.

Consent was granted on a short-term basis for the three established disposal sites in December 2013, to allow for modelling and monitoring for a long term renewal application to be carried out. The existing short-term consent relates to the 81 hectares of coastal marine space across the three historical disposal areas of Heyward Point, Aramoana and Shelly Beach.

Port Otago is seeking a long term (35-year) consent for its inshore dredging disposal activity. The modelling and monitoring required as a condition of the current disposal consent support a recommendation to extend the Heyward's site in order to provide for the disposal activity over the next 35 years. The extension is required to allow for adaptive management of disposal activities, particularly in terms of effects on surf breaks identified as nationally significant in the New Zealand Coastal Policy Statement 2010.

The consent to be sought is for the disposal into the sea of up to 450,000m^3 per year of dredged material derived from dredging the channel and berth areas in and about the Otago Harbour. The area subject to disposal activities will increase to incorporate an enlarged Heyward's site of 225 hectares, bringing the total area for the disposal activity to 268 hectares. The existing and proposed new grounds are shown in Figure 1.1.

The present report focuses on the characteristics of the plumes associated with sediment disposal within the new proposed ground. Methods employed for the hydrodynamic and particle tracking modelling are described in Section 2 and results are presented in Section 3. Section 4 concludes the report and references are included in Section 5.

Figure 1.1 Aerial photograph of the Otago Harbour Entrance region. Existing disposal grounds are shown in white and the new proposed ground at Heyward Point is shown in red.

2. METHODS

2.1. Modelling approach

The disposal of sediment in the oceanic environment can be conceptualized as a mixing process developing in two phases. In the case of silt to fine sand dredging, the content of a loaded dredge consists of a highly concentrated mixture of sediment and water. Here, the bulk behaviour of the sediment mixture becomes dominant over the individual particle settling processes. When the dredge opens its bottom door for release, the content will typically be released as a jet-like sediment flux quickly descending to the seabed. This sediment flux feature will impact the seabed and disperse radially in the lower 15-20% of the water column with rapid energy dissipation and settlement, typically over length scales of order O(100) m. This entire process is generally known as the dynamic plume phase (e.g. Spearman, J. et al., 2007). During the sediment load descent, some sediment will be stripped from the outside of the jet-like sediment feature and become suspended in the water column. In addition, the impact of the bulk sediment load on the seabed can also suspend or re-suspend sediment from the upper seabed layer. That suspended sediment load becomes subject to advection by the ambient flow and diffusion - form what is referred to as the passive plume (Figure 2.1)

In the present study, the focus is on the extent and concentration of the passive plume and its associated deposition. In general, the dynamic plume will include a dominant proportion of the total sediment load released. It is generally expected that only 2-5 %of the total volume of fine material is stripped from the dynamic plume to become suspended in the water column (EPA-USACE, 1998). Field data collected by Bokuniewicz et al. (1978) suggests even lower fractions, of the order 1%. That fraction was found to be slightly larger in some recent model simulations by Aarninkhof, S. and Luijendijk, A., (2009) which found that ~10% of the total load was entrained in the water column within the passive plume, while the 90% remaining formed a dynamic plume that settled quickly to the seabed. This slightly larger percentage is consistent with observations in Spearman et. al. (2011) as well as the default range suggested for use with the TASS model (5-15%) (HR Wallingford, 2010), although these concern the overflow discharge rather than discrete full load release.

Furthermore, the sediment stripping from the dynamic plume is expected to occur throughout the water column as the dynamic plume settles. The resulting suspended load may then combine with some suspended sediment in the lower water column due to the dynamic plume collapse. In the present application it was chosen to release particles at the bottom of the dredger hull, which is the initial point of contact of sediment with the receiving waters (2 m below sea surface for New Era, and 8 m for a large TSH dredger). Although strongly simplified, this approach ensures conservative predictions of the plume dispersion since particles may disperse for a longer time that they possibly would in reality when stripped deeper in the water column.

With respect to the timing of the operation, the sediment disposal is a process that is finite in time (i.e. occurring at a specific time, over a finite period) and inherently non-deterministic (i.e. controlled by random and

unpredictable variables such as currents and turbulences). Since future ocean conditions and exact timing of the disposals are unknown, it is not possible to predict the actual outcomes of a release before the event occurs. However, the probability of future oceanic conditions can be assessed from the historical conditions, thereby allowing "probabilistic" estimations of the geographical dispersion and deposition patterns. In the present study, it was decided to simulate sediment releases from the New Era or TSHD vessels continuously over a year-long simulation (2012) to include the potential ambient forcing variability on an annual timescale and thus produce robust probabilistic patterns of dispersion.

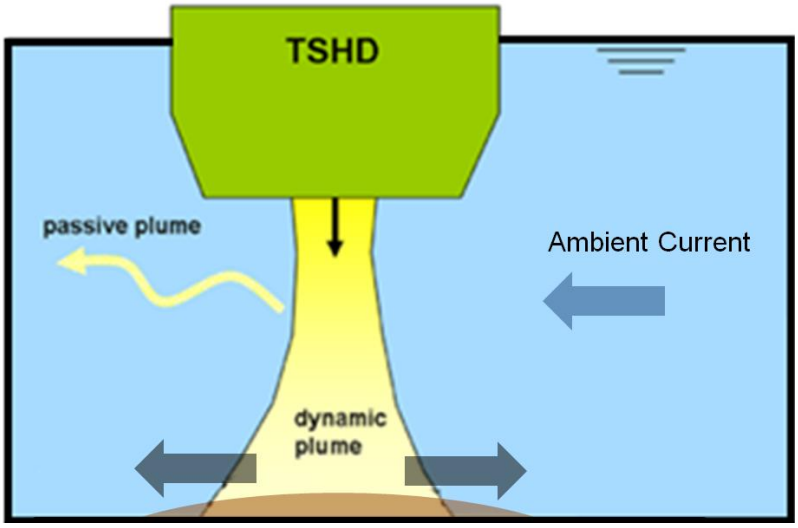

Figure 2.1 Sketch of processes following dredger sediment load release (modified from Aarninkhof, S. and Luijendijk, A., 2009).

2.2. Hydrodynamics

All the particle tracking simulations were undertaken using a 2-dimensional hindcast of the hydrodynamics of the Otago Peninsula region for the year 2012, simulated with the MSL implementation of the Princeton Ocean Model (POM). POM is a primitive equation ocean model that numerically solves for oceanic current motions. This model has been used for numerous scientific applications studying oceanic and shelf circulation. Details of POM implementations are described by Mellor (2004).

For the hindcast simulations, MSL-POM was used in a vertically-integrated two-dimensional mode on nested domains starting from the New Zealand MetOcean current hindcast (~6 km resolution), down to 1 km over the wider Otago region and ~150 m in the vicinity of the Otago Peninsula. Particle-tracking simulations were run using the high resolution domain. Medium and high resolution grids are shown in Figure 2.2. For the New Zealand scale model, the same boundary conditions were applied at all open boundaries. For the surface elevation, an Orlanski (1976) type radiation boundary condition was applied, but with the normal component of the outgoing phase speed determined as the normal projection of the full oblique phase speed (NPO in Marchesiello *et al*., 2001). For the normal component of depth-averaged velocity, a Flather (1976) type constraint was used. The TPXO7.2 global inverse tidal solution (Egbert and Erofeeva, 2002) was used to prescribe the tidal elevation and current velocity at the boundaries of the New Zealand grid.

The surface wind fields used were sourced from a 35-year regional atmospheric hindcast run using an implementation of the WRF (Weather Research and Forecasting) model established over all New Zealand at 12 km resolution. The WRF model boundaries were prescribed from the CFSR (Climate Forecast System Reanalysis) dataset distributed by NOAA (Saha et al., 2010). These data span 35 years (1979-2013) at hourly intervals and 0.31° spatial resolution.

The MSL-POM current model has been validated at various coastal and open-ocean locations around New Zealand, including North and South Taranaki, Western Cook Strait and the Bay of Plenty. A specific validation exercise was undertaken for the Otago Peninsula region using measured currents at the A0 site over a 3 month period (see MSL report P0140-03).

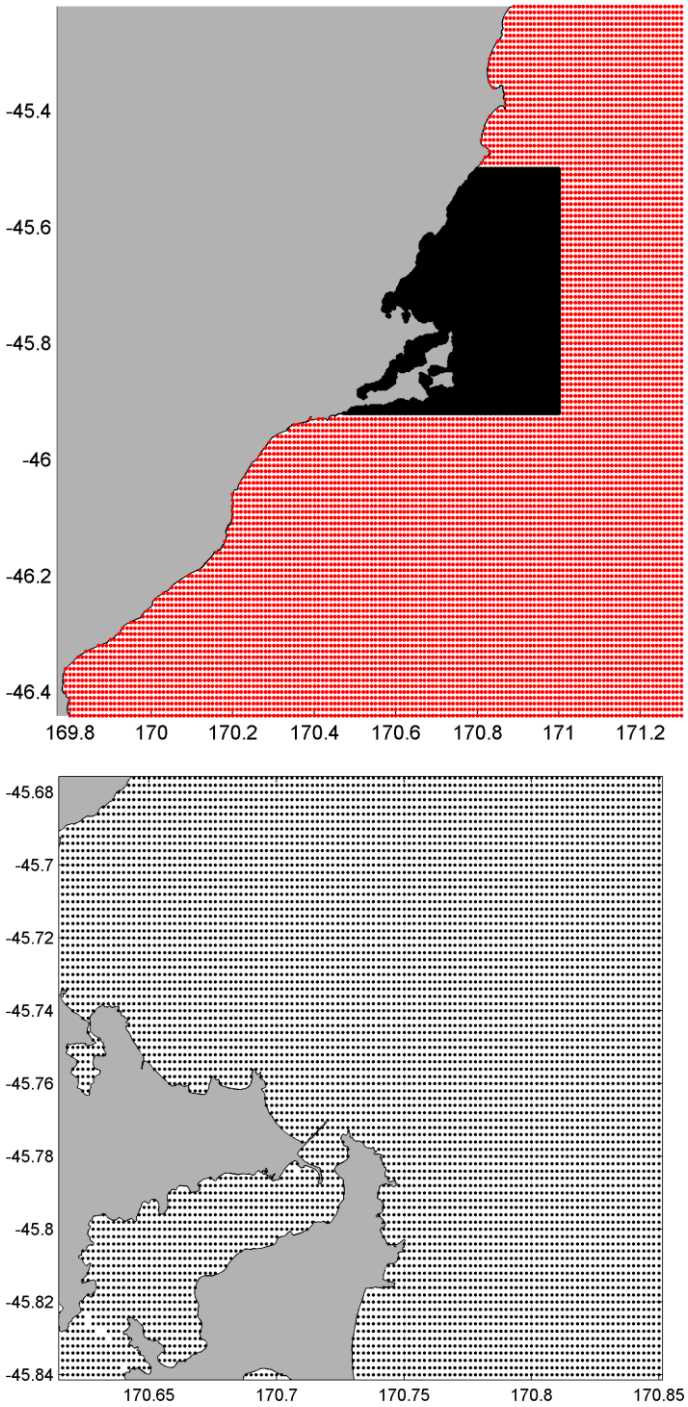

Figure 2.2 Medium and high resolution grids of the MSL-POM hydrodynamic hindcast (1 km and ~150 m resolution respectively). The bottom picture is a zoomed-in view of the high resolution grid which was used for the particle tracking simulations in the vicinity of the Otago Harbour Entrance.

2.3. Trajectory modelling

2.3.1. Particle-tracking model

A Lagrangian model developed by MSL was used to simulate the trajectories of particles released at the considered disposal sites. The model consists of trajectory scheme applied here to the 2D Eulerian current field $(\tilde{u},\tilde{v})$ (see section 2.2), solving for the motion of discrete particles.

$$\frac{du_p}{dt} = \tilde{u}(x,y,z,t) + u_t$$
$$\frac{dv_p}{dt} = \tilde{v}(x,y,z,t) + v_t \qquad \text{(2.1 a,b,c)}$$
$$\frac{dw_p}{dt} = -w_s + w_g + w_t$$

where (u_t , v_t, w_t) are the diffusion components representing turbulent motions, w_s is the particle settling velocity and w_g is a vertical velocity component accounting for bathymetric gradients.

In the horizontal plane, the model uses an Ordinary Differential Equations (ODE) solver, including a 4th order Runge-Kutta method, to calculate the trajectory of a given particle (u_p,v_p) in the time-varying derivative field.

Diffusion is treated using a random walk approach with the following equation, shown for the u_t component:

$$\int_t^{t+\Delta t} u_t . dt = \sqrt{6 . k_{u,v} . \Delta t} \; . \theta(-1,1) \qquad (2.2)$$

where $\theta(-1,1)$ is a random number from a uniform distribution between -1 and 1, Δt is the time step of the model in seconds and $k_{u,v}$ is the horizontal eddy diffusivity coefficient in $m^2.s^{-1}$.

In absence of specific field data, the determination of the diffusion coefficient $k_{u,v}$ is generally based on empirical relationships. For dispersion at oceanic scales, Okubo (1971) notably showed that $k_{u,v}$ varies approximately (with wide scatter) as :

$$k_{u,v} = \alpha . L^{4/3} \qquad (2.3)$$

where L is the horizontal scale of the mixing phenomena.

Furthermore, in numerical models, the role of the horizontal diffusion coefficient is also to implicitly account for sub-gridscale turbulent processes such as eddies that are not explicitly resolved in the model due to the limited resolution. This means that horizontal diffusion must generally increase as grid size increases since eddies of increasing scale are unrepresented. On the contrary, the reduction of grid size allows explicit resolution of flow patterns and eddies at finer scales which thereby reduce the required amount of added diffusion.

The high resolution hydrodynamic grid to be used for the particle tracking simulations has a grid size of ~ 150 m, which yields a range of diffusivities of $0.04 < k_{u,v} < 0.36$ $m^2.s^{-1}$ according to the various diagrams provided in Okubo (1971). Here, a generic value of 0.1 $m^2.s^{-1}$ was eventually chosen for the following model simulations.

The trajectory of particles in the vertical plane is controlled by the particle's settling velocity w_s, the vertical diffusion component w_t as defined in equation 2.1c with a constant vertical eddy diffusivity coefficient k_w of 0.0001 $m^2.s^{-1}$, and a component w_g related to the bathymetric gradient to ensure that the trajectory of a particle close to the sea-floor is parallel to it (before settling and diffusion components are applied):

$$w_g = \frac{(h-z)}{h}\left(\tilde{u}(x,y,z,t)\times\frac{dh}{dx}+\tilde{v}(x,y,z,t)\times\frac{dh}{dy}\right) \qquad (2.4)$$

where z is the particle elevation above the seabed, h is the water-column height at the particles' horizontal location (x,y), $(\tilde{u},\tilde{v})$ is the 2D current field from equation 2.1 and $\left(\frac{dh}{dx},\frac{dh}{dy}\right)$ is the bathymetry gradient. Note a logarithmic profile was used to extrapolate the 2D depth-averaged current magnitudes to any water column level.

In the present model implementation, any particle reaching the shoreline, the seabed or the outside domain boundaries remained at the position of intersection (*i.e.* 'sticky' boundaries), thus allowing no sediment re-suspension.

2.3.2. Particle sizes and release scenarios

Information on the distribution of the sediment to be dredged provided by Port Otago indicates two dominant types of sediment, namely medium to fine sand and silt. Any material larger than fine sand is expected to have a very limited effect on the passive plume since it would settle very quickly (e.g. vertical settling of ~ 10 m per 5 minutes for a d_{50} of 300 µm). For the model simulations, the sediment to be disposed was therefore modelled as two representative size classes, fine sand and silt.

A set of sediment samples obtained at several locations within the Harbour suggests a relatively consistent median grain size d_{50} of ~ 200 µm for the sand fraction. Associated settling velocity was computed using equation by Van Rijn (1993) for the non-cohesive regime yielding 0.0220 m/s. It is noted that even this fine sand fraction will settle relatively quickly to the seabed (e.g. vertical settling of ~ 10 m per 8 minutes).

Available samples for the silt material indicate median grain sizes d_{50} ranging from ~9 to 40 µm, generally centred around 20 µm. Silt is a cohesive material in which individual particles tend to bond together to form larger particle aggregates or “flocs”, which will increase settling rates and thus reduce the time they remain in suspension. The formation of such flocs is a complex process which depends on numerous parameters including nature of sediment, concentration in dredger load, ambient salinity etc. In general, settling velocities of cohesive particle aggregates

can be expected to be of order 0.1-10 mm/s (e.g. Berlamont et al., 1993). In the absence of information on the in-situ characteristics of the sediment mixture within the dredger, it was assumed that particles of the representative silt class would flocculate to ~40 µm, which is the upper end of the measured range. This diameter was used for the determination of the settling velocity using again equations of Van Rijn (1993) and yielded a settling rate of ~ 1 mm/s. Note this settling rate is consistent with recent observations made on flocculated sediment loads in TSHD (Smith and Friedrichs, 2011).

The release characteristics of these two particle classes were varied based on the two potential dredgers likely to be used for the dredging/disposal operations. They are:

- A large trailing suction hopper dredger (TSHD) with a release depth at approximately 7 m below surface, and a total volume per hopper load of 22,000 m^3.

- A smaller dredger called New Era used at Port Otago with a release depth at approximately 2 m below surface, and a total volume per hopper load of 600 m^3.

Here, it is chosen to release sediment at the bottom of the dredger hull. This is a conservative choice since, in reality, the sediment stripping from the dynamic plume and suspension into ambient waters will develop throughout the entire vertical water column, therefore reducing the vertical settling distance and relative advection time before settling of some of the released sediment.

To cover the variability in the ambient hydrodynamic forcing throughout the ground, sediment was released at five sites within the proposed disposal ground (see Figure 2.3). Respective site depths are 23.5, 23.5, 14.0, 19.0 and 17.5 m, MSL. For comparison purposes, the dispersion results obtained for sites 3 and 4 are expected to be representative of the disposal activities inside the existing ground given their proximity.

Finally, it is noted that the results for the fine sand and silt classes can essentially be interpreted as the smallest and largest plume footprints expected during the disposal activities. Indeed a dredger of load of sand-only would produce very compact SSC and deposition patterns due the rapid settling of the sediment while a dredger load of silt-only would produce much more extended spatial spreading of the sediment because of the slower settling. In practice, the dredger content will typically be a mixture of both sand and silt materials however these two sets of results (i.e. fine sand and silt) do provide a spatial bounding of the dispersion expected.

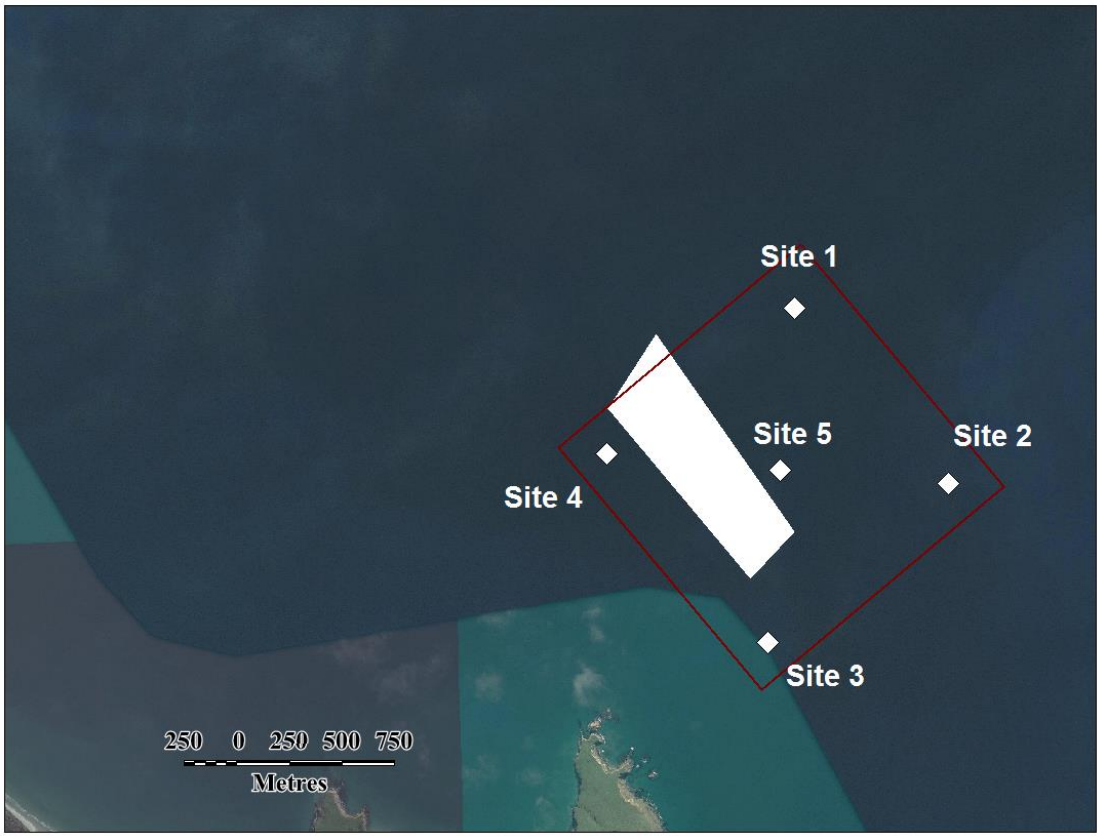

Figure 2.3 Release sites (white dots) considered within the proposed Heyward Point disposal ground (shown in red). The existing disposal ground is shown in white.

2.3.3. Post-processing

The results of the particle tracking simulations were post-processed to produce concentration and deposition spatial fields as well as probabilistic footprints of the particle cloud dispersion and deposition.

The general methods employed to reconstruct particle concentration fields from the particle-tracking model outputs are outlined below. To reduce the 1-year particle-tracking model outputs to a robust picture of the dispersion patterns, concentrations were computed from overall particle clouds combining all suspended (or deposited) particle positions after a 12 h time period. Note the maximum particle age at settling was generally up to ~ 9 hours for the silt fraction (i.e. smaller settling velocities). The effective maximum particle age at settling will depend on the sediment type, site and depth of release, ambient conditions during release as well as direction of initial dispersion (e.g. connection towards deeper regions or different flow features).

To reconstruct concentrations from the particle clouds at chosen receptors, a kernel method with variable bandwidth was used. The use of a variable bandwidth (kernel size) attempts to represent true variability of spatial concentration, while minimizing statistical variability that inevitably occurs away from the source due to a necessarily finite number of particles. A small kernel is used in regions gathering a high number of particles, where it is statistically appropriate to infer relatively small scale changes in concentration. Conversely, a larger kernel is used in regions presenting a

low number of particles, so as to prevent unrealistically high concentrations around the precise (but partially random) locations of a few isolated particles.

In practice, the concentration C at a given receptor location (x,y) is computed as:

$$C(x,y) = \sum_{i=1}^{n} \frac{m_i}{\lambda_x(x,y)\lambda_y(x,y)} K\left(\left|\frac{x_i - x}{\lambda_x}\right|\right) K\left(\left|\frac{y_i - y}{\lambda_y}\right|\right) \quad (2.5)$$

where (x_i,y_i) is the location of each particle i, n is the total number of particles, m_i is the loading for each particle, λ_x and λ_y are the kernel bandwidth in the x and y directions for location (x,y) and K is the kernel function.

Following Vitali et al. (2006), an Epanechnikov kernel function was used:

$$K(q) = \begin{cases} 0.75\left(1 - q^2\right), |q| \le 1 \\ 0 \qquad\qquad , |q| > 1 \end{cases} \quad (2.6)$$

where q is the ratio of the particle distance from receptor to bandwidth ($q_x=d_x/\lambda_x$, or $q_y=d_y/\lambda_y$)

A receptor-based method derived from the RL3 method in Vitali et al. (2006) was used to define the bandwidths λ_x and λ_y.

For each receptor location, a neighbourhood was defined as the region enclosing the 1/20th closest particles. Then, for each direction x and y, the bandwidths λ_x and λ_y were defined as the minimum value between the maximum projected distance of the particles within the neighbourhood and twice the standard deviation of the projected distances within the neighbourhood. Finally, in order to prevent unrealistically elongated kernels, the aspect ratio λ_x / λ_y was limited to be no greater than 5:1, with the smaller value increased.

The loading of each particle m_i directly depends on the material being modeled. To get an initial picture of the dispersion characteristics, concentrations were initially computed attributing a constant arbitrary load to each particle. Obtained concentrations were then normalized by the maximum concentration magnitude to provide relative concentrations fields. The interest of these fields is that they can be scaled to any true quantity of sediment released.

The receptor grid used for the concentration computation is independent of the hydrodynamic grid and allows focusing resolution in the region of interest. The concentration grid used here grid had element sizes ranging from 1000 m offshore to 60 m in the vicinity of the ground and Harbour Entrance region (Figure 2.4).

Note that the term concentration refers here to either concentrations of suspended particle concentrations when computed from the suspended particle clouds or concentrations of deposited particles (i.e. depositional thickness) when computed from the deposited particles.

Besides concentration fields, simulation results were also analyzed to produce probabilistic particle excursion footprints. These contours allow spatially quantifying the probabilities of finding particles around the release location. The excursion contours are defined by first computing all the particle distances from release and then defining a range of distance statistics (e.g. percentiles) in each directional sector around the release location. For a given percentile level X, the excursion distances in each directional bins form a contour around the release location which can be interpreted as the spatial footprint including X % of all the particles. These contours were determined from the same particle clouds as used in the concentration computations (i.e. after 12 hours) for three percentile levels of 90, 95 and 99th of the distance release-particles. Contours at these high percentile levels allow the definition of the total region of influence of the disposal activities. The maximum distances are purposely not included to avoid irrelevant polygon skewness due to individual outliers. Note this method is adequate for relatively open spaces with limited land obstructions in the directional sectors around the release.

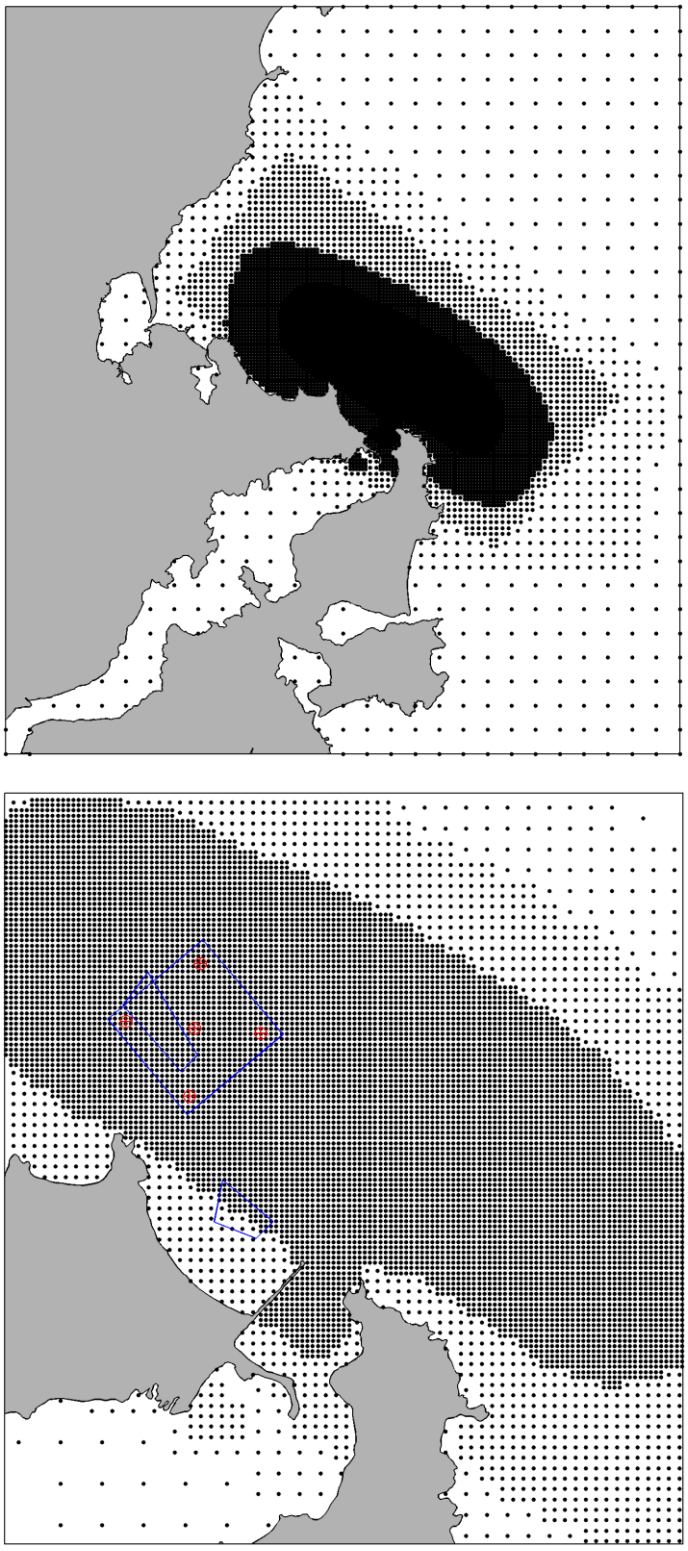

Figure 2.4 Receptor grid used for particle concentration computation. The resolution ranges from 1000 m offshore to 60 m in the vicinity of the ground and Harbour Entrance region. The existing and proposed disposal grounds are shown in blue and considered release sites are shown in red.

3. RESULTS

3.1. Hydrodynamics at the release sites

Tidal and residual current roses at the five release sites within the proposed Heyward Point disposal ground (Figure 2.3) are shown in Figure 3.1 and Figure 3.2.

Comparison of current roses indicates the local hydrodynamic regime is dominated by residual circulation and mostly bi-modal with northwest or southeast-directed flows. Although the current climate further offshore is expected to be influenced by the north-directed flows of the Southland Current which is a geostrophic current flowing northward off the eastern coast of the south island of New Zealand, the local hydrodynamic regime is clearly dominated by southeast-directed flows. As mentioned in MSL report P0140-03, this can be attributed to the formation of a meso-scale counter-clockwise eddy in the wider Blueskin Bay. Mean residual velocities are southeast-directed and around ~0.1 m/s through the sites, with maximum velocities of order 0.5 m/s. Site 3 is the most energetic site and this can be related to the proximity of the Heyward Point which locally focuses ambient flows as well as its shallower water depth (~14 m, MSL).

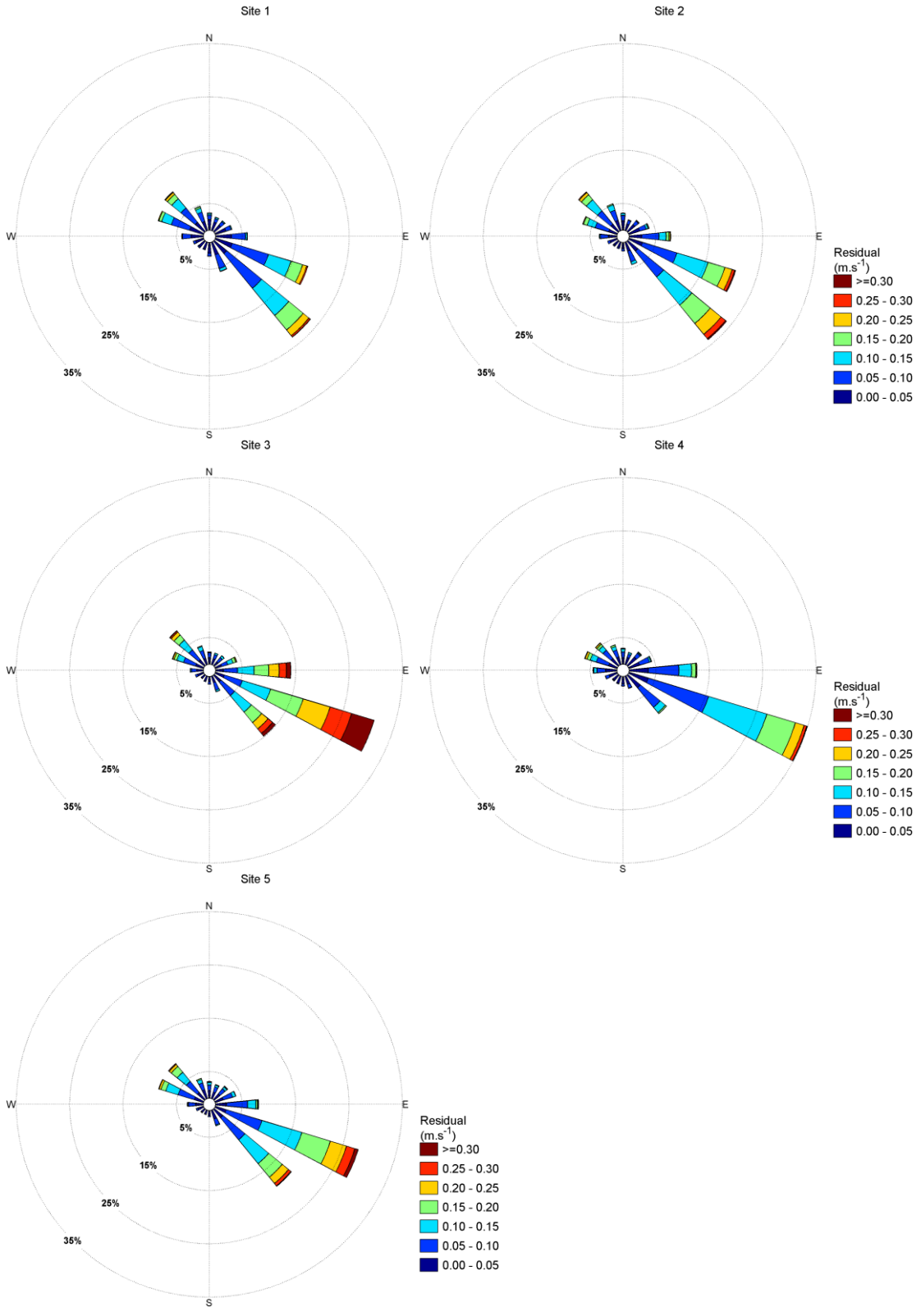

Figure 3.1 Residual current roses at release sites shown in Figure 2.3.

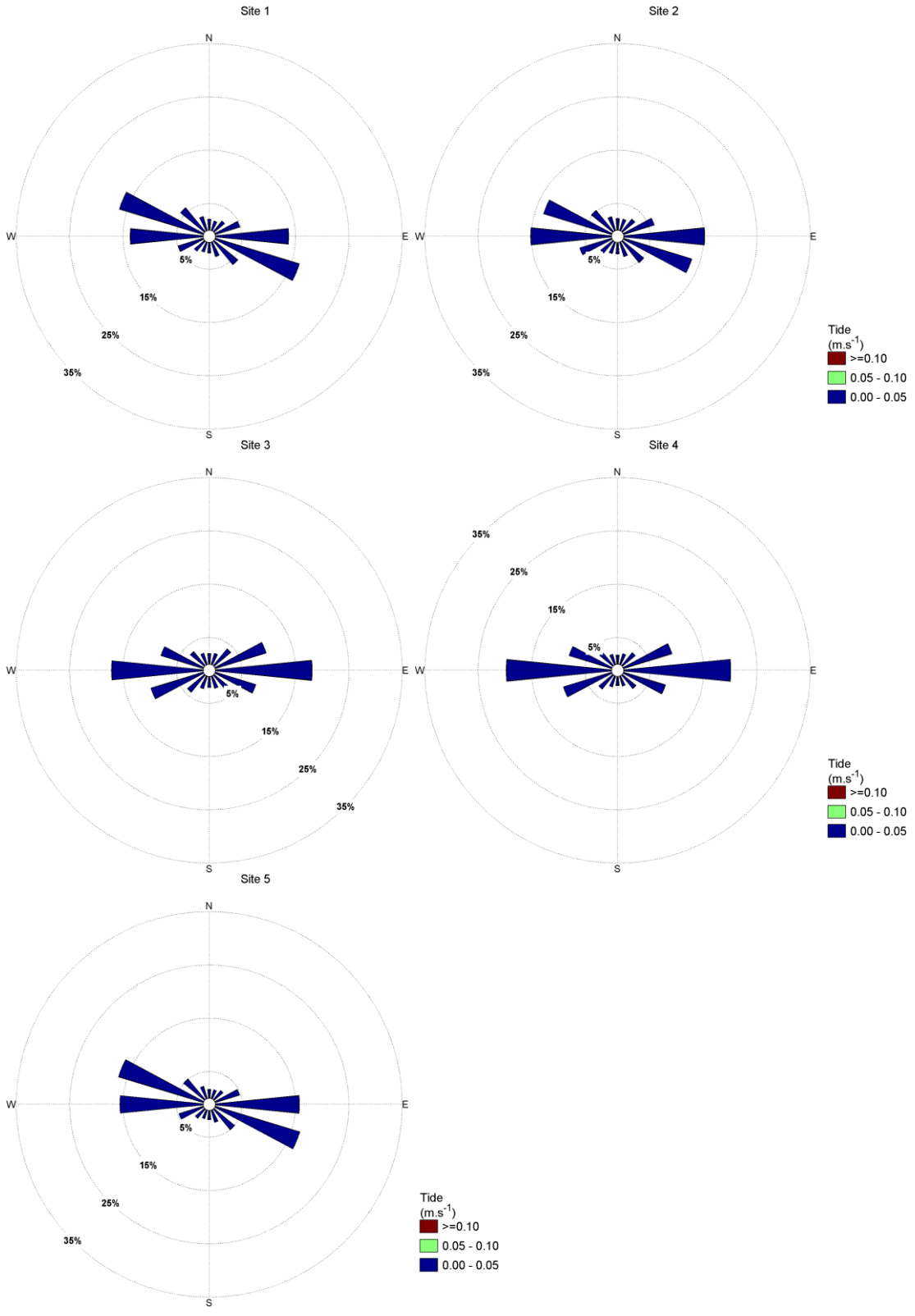

Figure 3.2 Tidal current roses at release sites shown in Figure 2.3.

3.2. Suspended sediment concentration (SSC) fields

Maps of the mean normalized SSC are shown in Figure 3.3 to Figure 3.8 for the 5 five release site considered. It is reminded that these normalized concentrations do not give information of the actual suspended sediment concentration (SSC) levels. Instead they provide a picture of the relative SSC spatial distribution within the passive plume both in the horizontal as well as in the vertical (i.e. SSC computed at three levels in the water column).

Note results for the fine-sand fraction are only included for site 1 in Figure 3.4. It is clearly seen that the relatively large settling rate of the fine-sand class results in very limited plume dispersion. The fine-sand SSC maps were therefore not reproduced for the other sites.

As expected given the ambient flows (see section 3.1), the general SSC predicted for the silt fraction follow an axis northwest-southeast, with a larger skewness towards the southeast. Note the general plume asymmetry towards the southeast results in the plume crossing the channel region to various degrees depending on the actual release site and depth.

For the New Era dredger with a relatively shallow release (2 m below surface), the SSC plume is the most concentrated in the surface level (highest 3 m of water column) but with limited extents (300-500 m). The plume widens in deeper levels as particles settle and are advected by ambient currents, conserving an elongated shape. For a TSHD dredger, relative SSC levels are insignificant in the surface layer. Here the maximum concentrations are found mid-water which is due to the deeper release (7 m below surface). Overall patterns are consistent with the New Era cases but general extents are smaller because the deeper release relatively reduces the time period during which particles are advected before settling.

It is noted that despite the apparent impact reduction for the TSHD case, in reality actual quantities of released sediment will be much more significant that these released by the New Era. As a result, actual SSC levels during events of TSHD disposal will most likely be associated with SSC levels one of several orders of magnitudes larger than during New Era-disposal events.

Summary SSC fields combining results for all release sites are included in Figure 3.9 and Figure 3.10 for silt and fine sand respectively (i.e. largest and smallest dispersions expected).

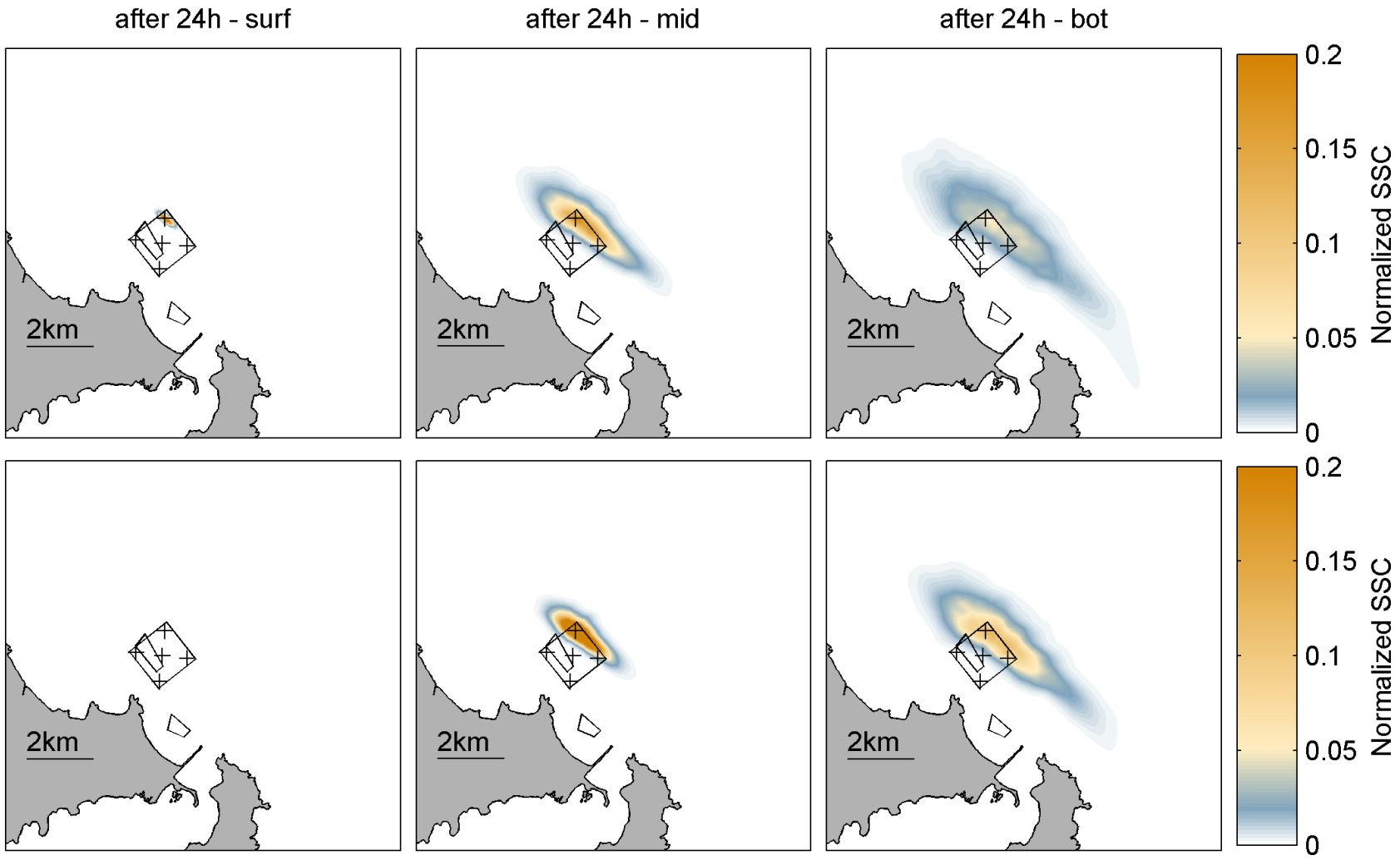

Figure 3.3 Normalized SSC at three levels in the water column for a release of silt at site 1 (top: New Era, bottom: TSHD).

Figure 3.4 Normalized SSC at three levels in the water column for a release of fine-sand at site 1 (top: New Era, bottom: TSHD).

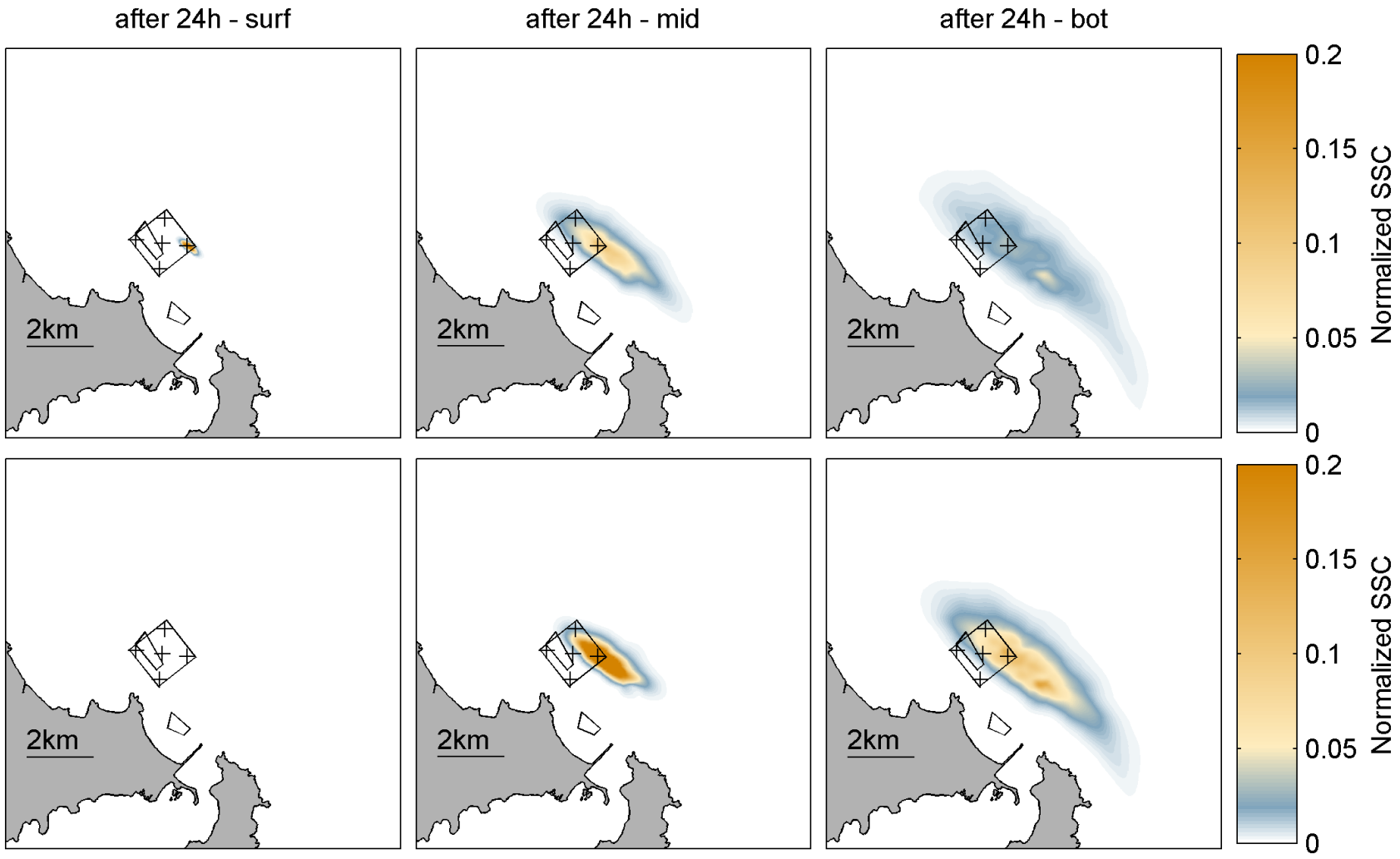

Figure 3.5 Normalized SSC at three levels in the water column for a release of silt at site 2 (top: New Era, bottom: TSHD).

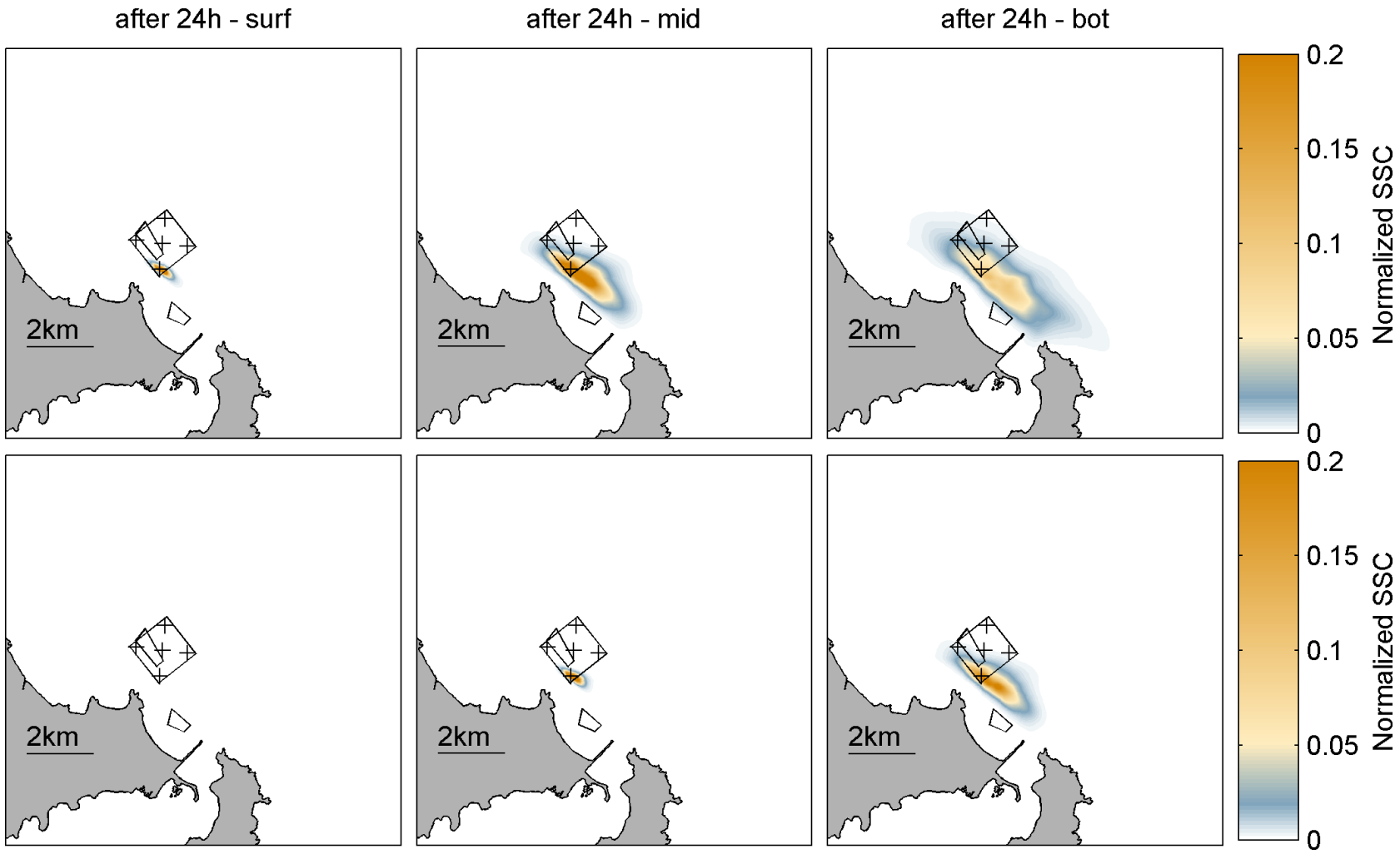

Figure 3.6 Normalized SSC at three levels in the water column for a release of silt at site 3 (top: New Era, bottom: TSHD).

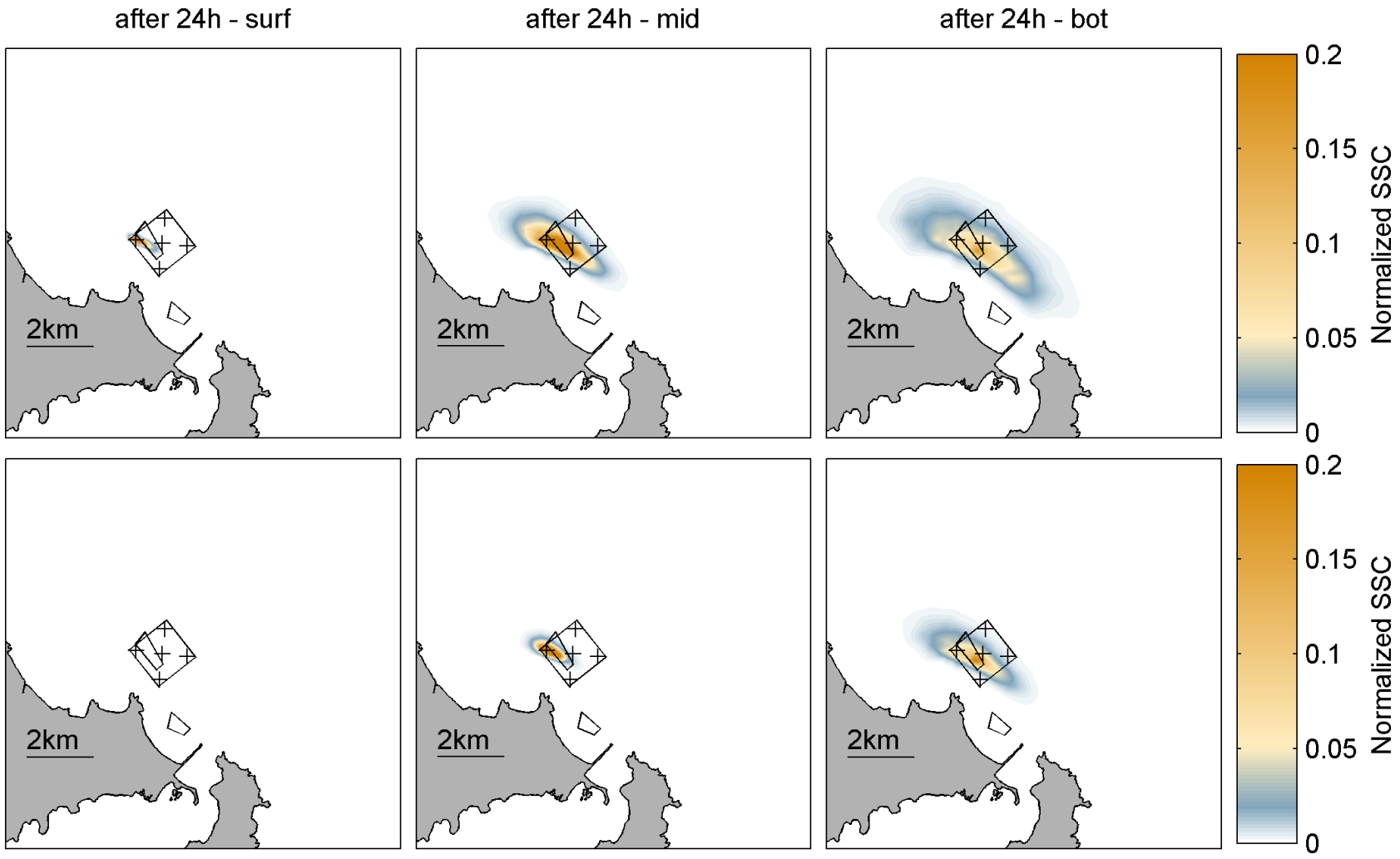

Figure 3.7 Normalized SSC at three levels in the water column for a release of silt at site 4 (top: New Era, bottom: TSHD).

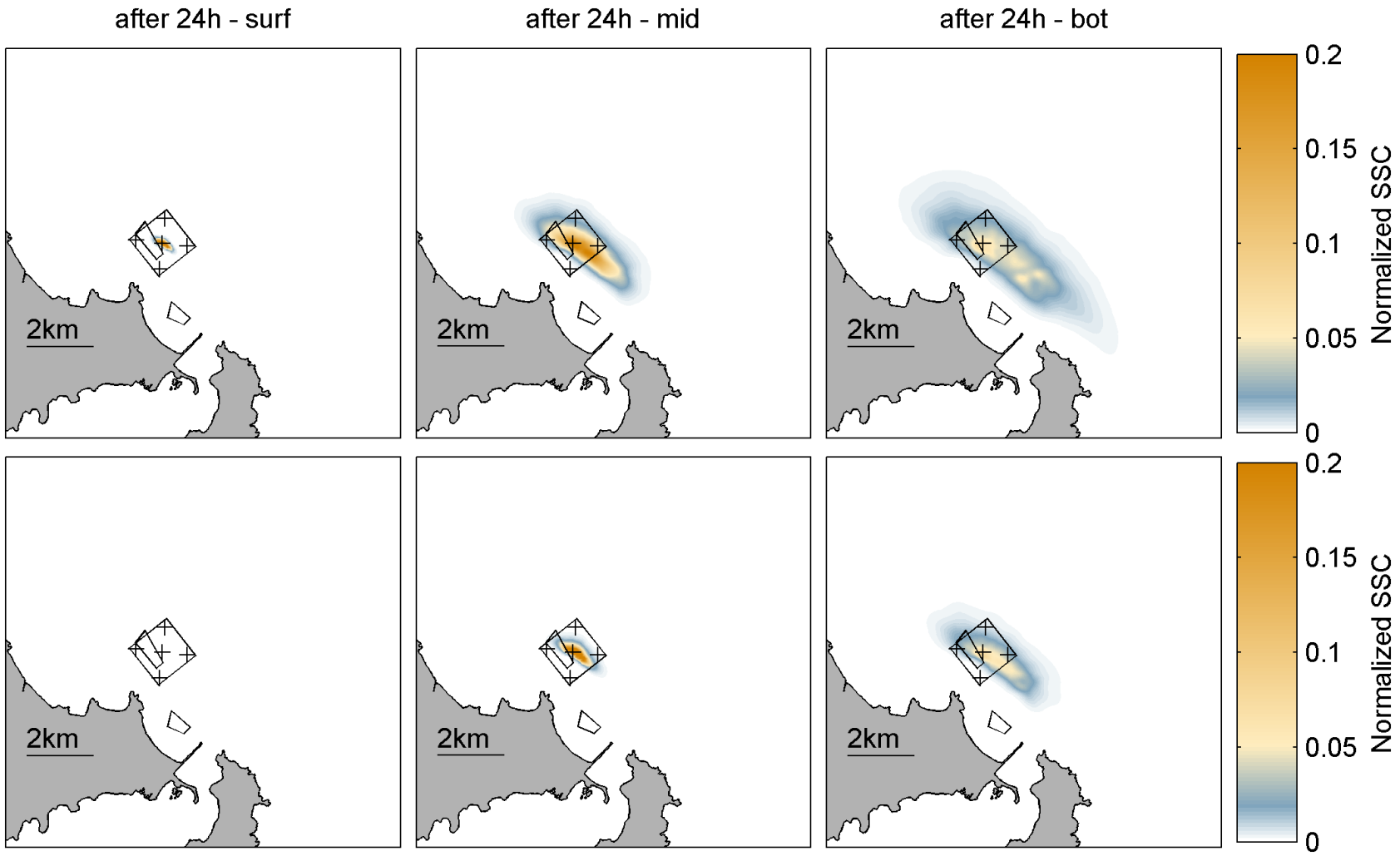

Figure 3.8 Normalized SSC at three levels in the water column for a release of silt at site 5 (top: New Era, bottom: TSHD).

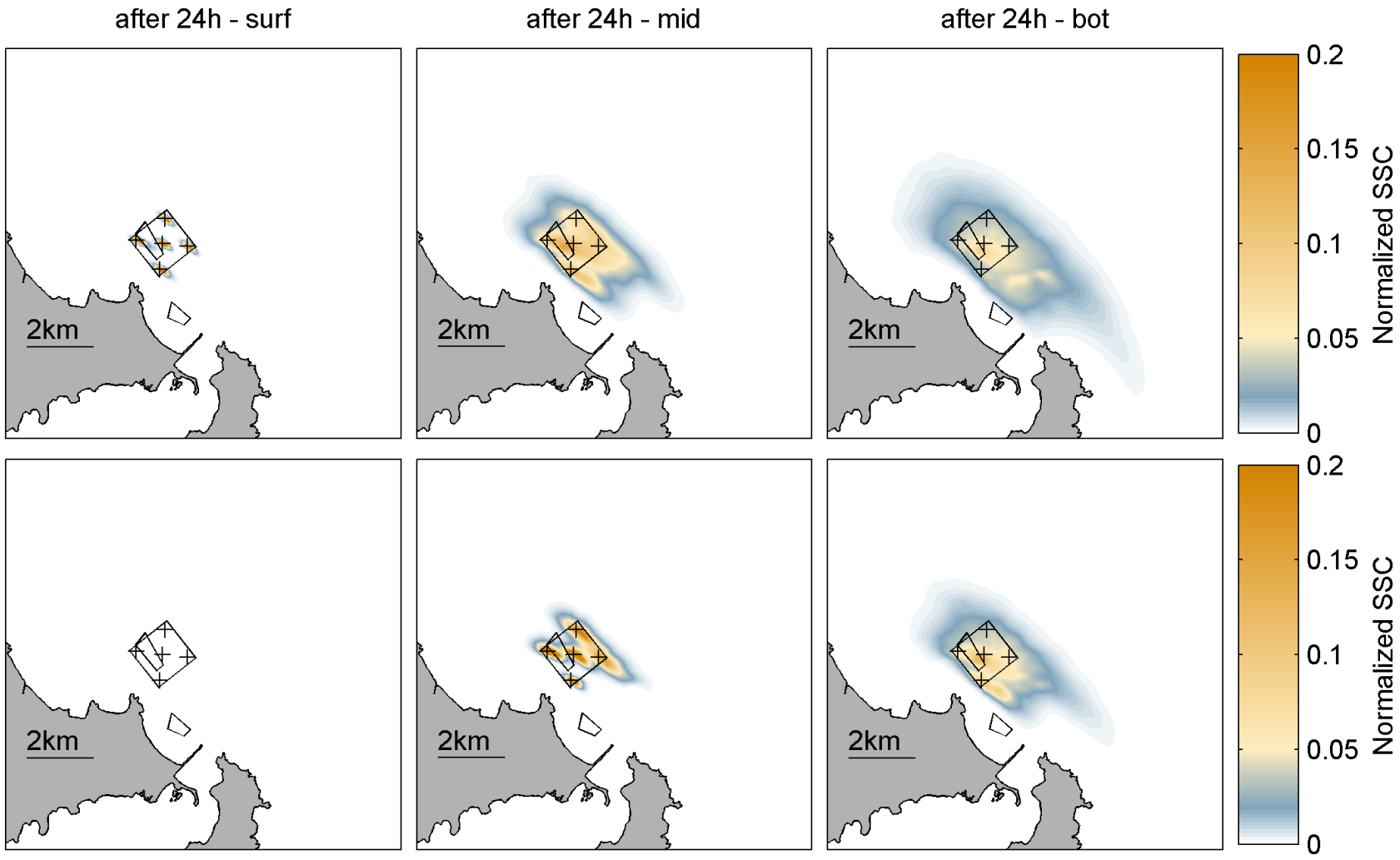

Figure 3.9 Normalized SSC at three levels in the water column for releases of silt at all sites (top: New Era, bottom: TSHD).

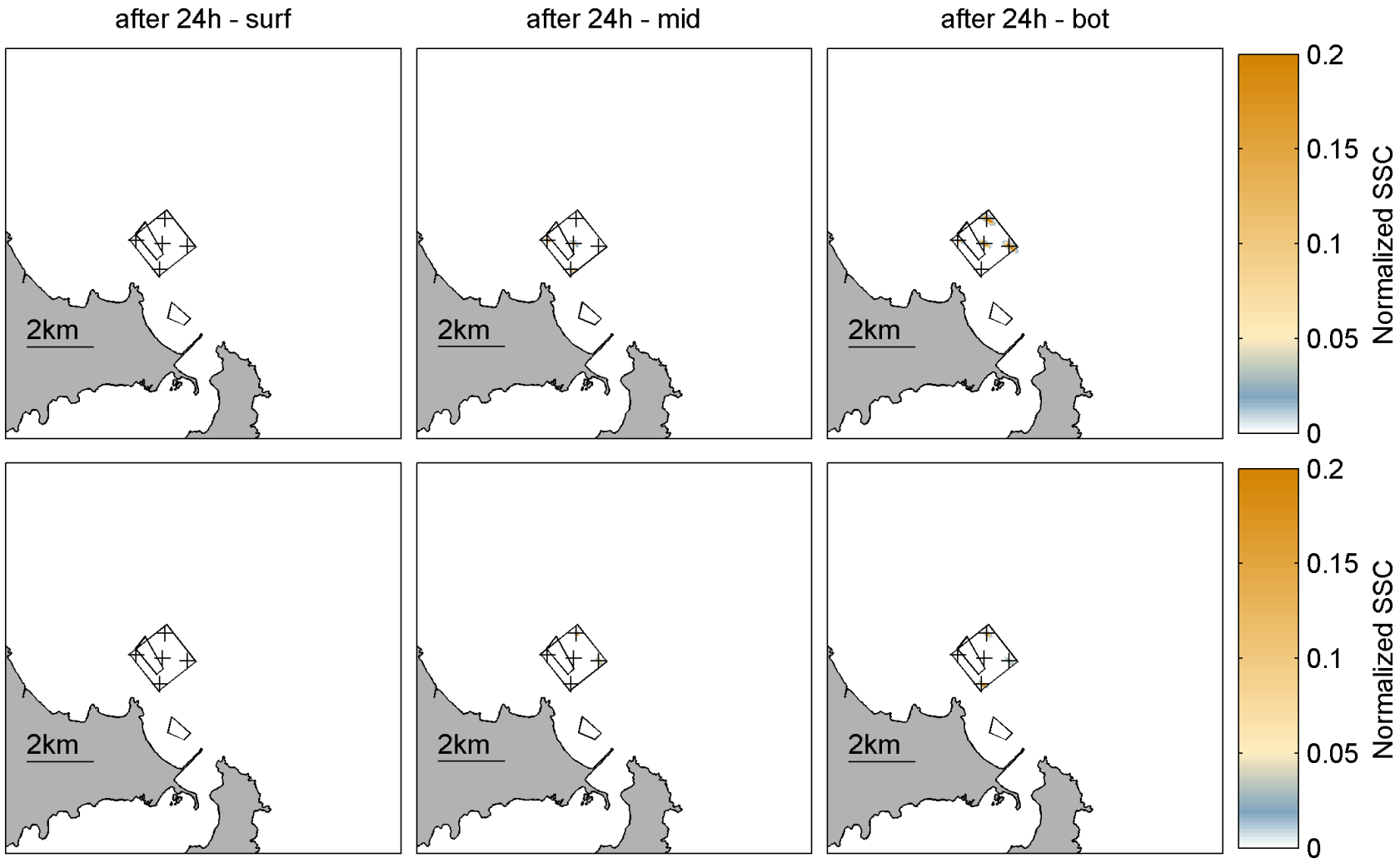

Figure 3.10 Normalized SSC at three levels in the water column for releases of fine sand at all sites (top: New Era, bottom: TSHD).

3.3. Deposition fields

Maps of the mean normalized deposition are shown in Figure 3.11 to Figure 3.16 for the five release sites simulated here. The fine sand results are presented only for site 1 given the limited extents of the deposition field around the release. It should be again noted that these normalized depositions do not give information on the actual deposition thickness. Instead they provide a picture of the spatial distribution of the deposition associated with the passive plume.

Consistent with the SSC plumes results, the deposition patterns are elongated in the northwest-southeast direction, with larger southeast excursions.

The release sites 1, 2 and 5 which are the farthest offshore general results in the largest deposition footprints with relative deposition dropping below 0.1 (i.e. less than 10 % of maximum deposition) ~1-2 km to the northwest and 2-4 km to the southeast. Inshore sites 3 and 4 exhibit more compact but also relatively thicker deposition patterns. Relative deposition footprints are again consistently more compact for the TSHD case that for the New Era case due to the deeper release. It is though reminded that the absolute deposition thicknesses are expected to be larger given the larger quantities of sediment likely involved during the TSHD-disposal events. Orders of magnitudes of the absolute thicknesses deposited can be estimated based on a given volume of sediment disposed. For example, assuming a full TSHD load of either fine sand or silt (i.e. 22,000 m^3) and that 10% of the disposed sediment is transferred in the passive plume, maximum thicknesses would or order 1-2 mm for silt, and 200-400 mm for sand. Note these should again be interpreted as an upper bound magnitude since the disposed sediment will typically be a mixture of both sediment types.

Notably, deposition footprints all connect with the channel region, with local sediment accumulation predicted near the channel end and tip of the submerged delta predicted for offshore sites 1, 2 and 5. Deposition is predicted to progressively move further south in the channel for the site 4 and 3 respectively, which suggests that a fraction of the disposed sediment, albeit very small, could eventually recirculate through the Harbour. However, the SSC levels in that region are expected to be very low (e.g. Figure 3.6, 0-5 % of maximum concentration).

Summary deposition fields combining results for all release sites are included in Figure 3.17 and Figure 3.18 for silt and fine sand respectively (i.e. largest and smallest dispersions expected).

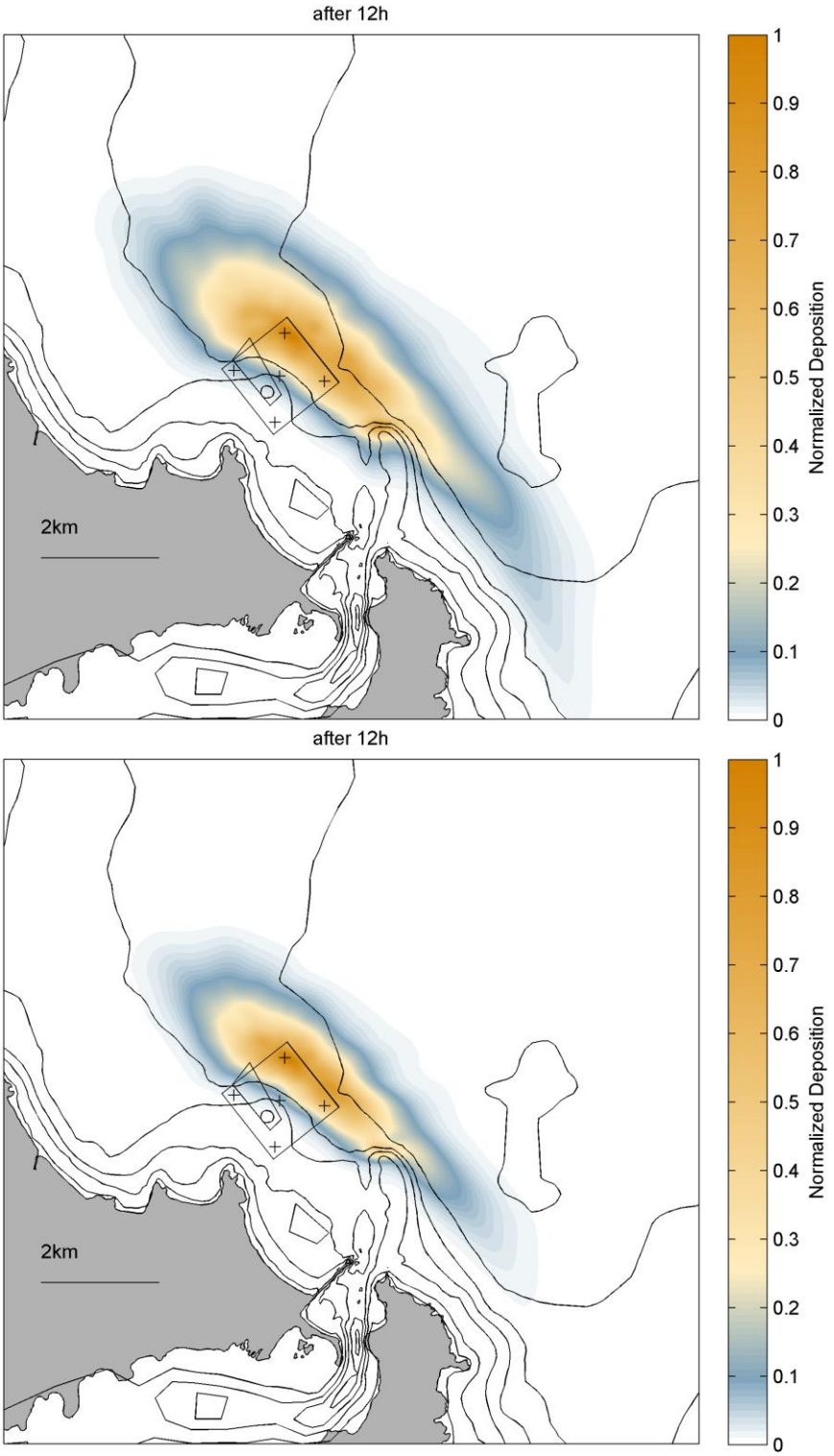

Figure 3.11 Normalized deposition for a release of silt at site 1 (top: New Era, bottom: TSHD).

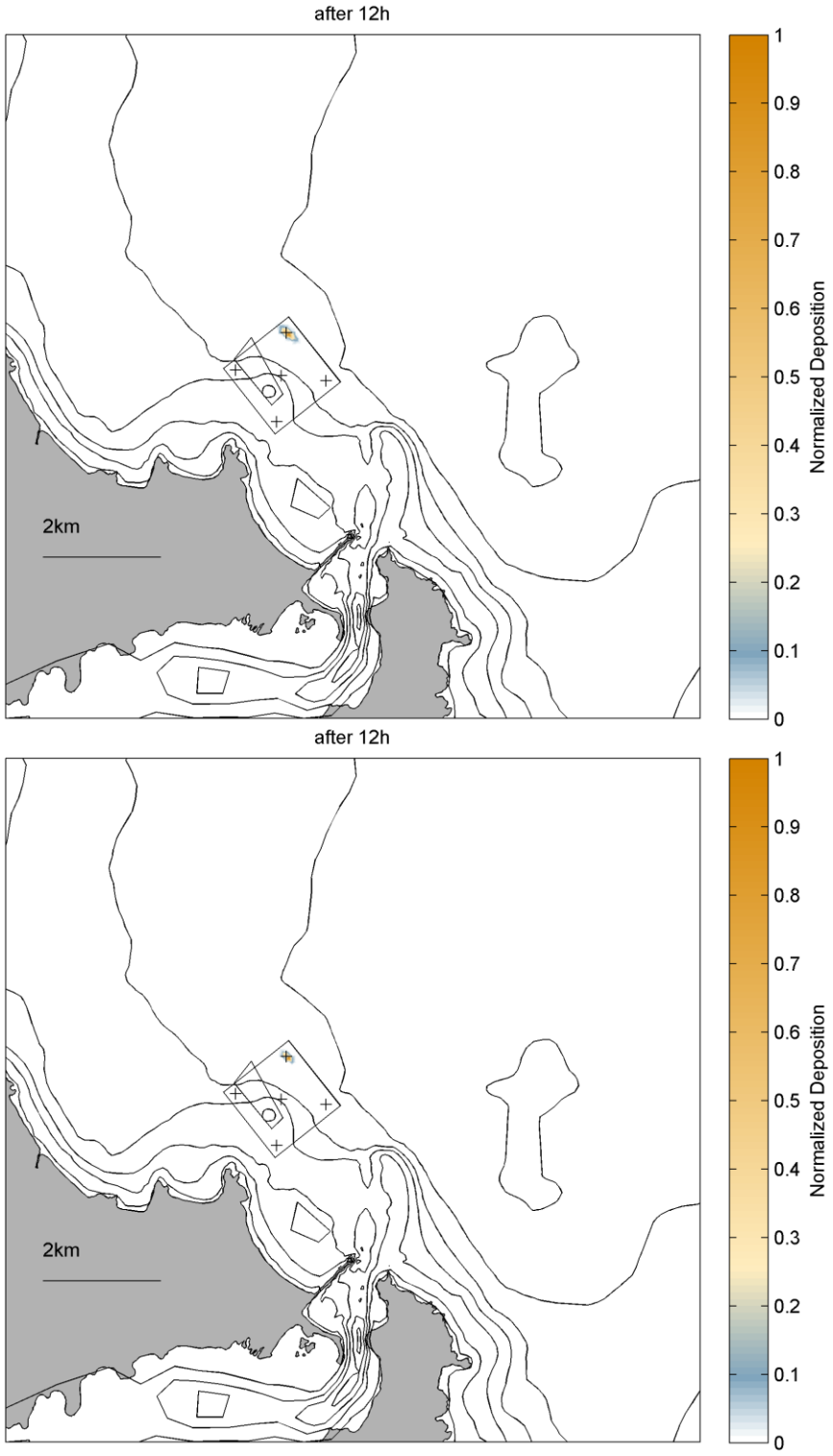

Figure 3.12 Normalized deposition for a release of fine-sand at site 1 (top: New Era, bottom: TSHD).

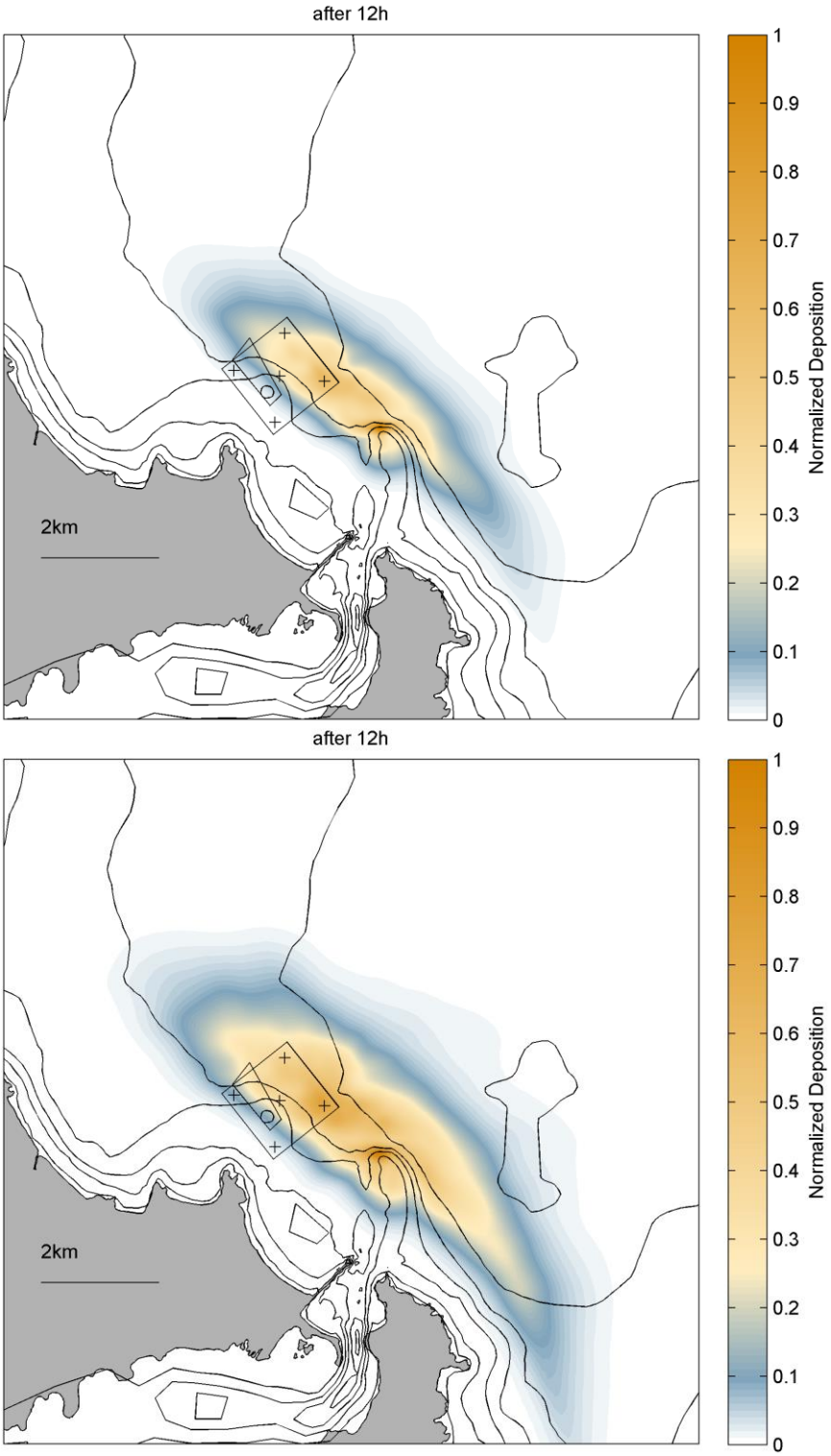

Figure 3.13 Normalized deposition for a release of silt at site 2 (top: New Era, bottom: TSHD).

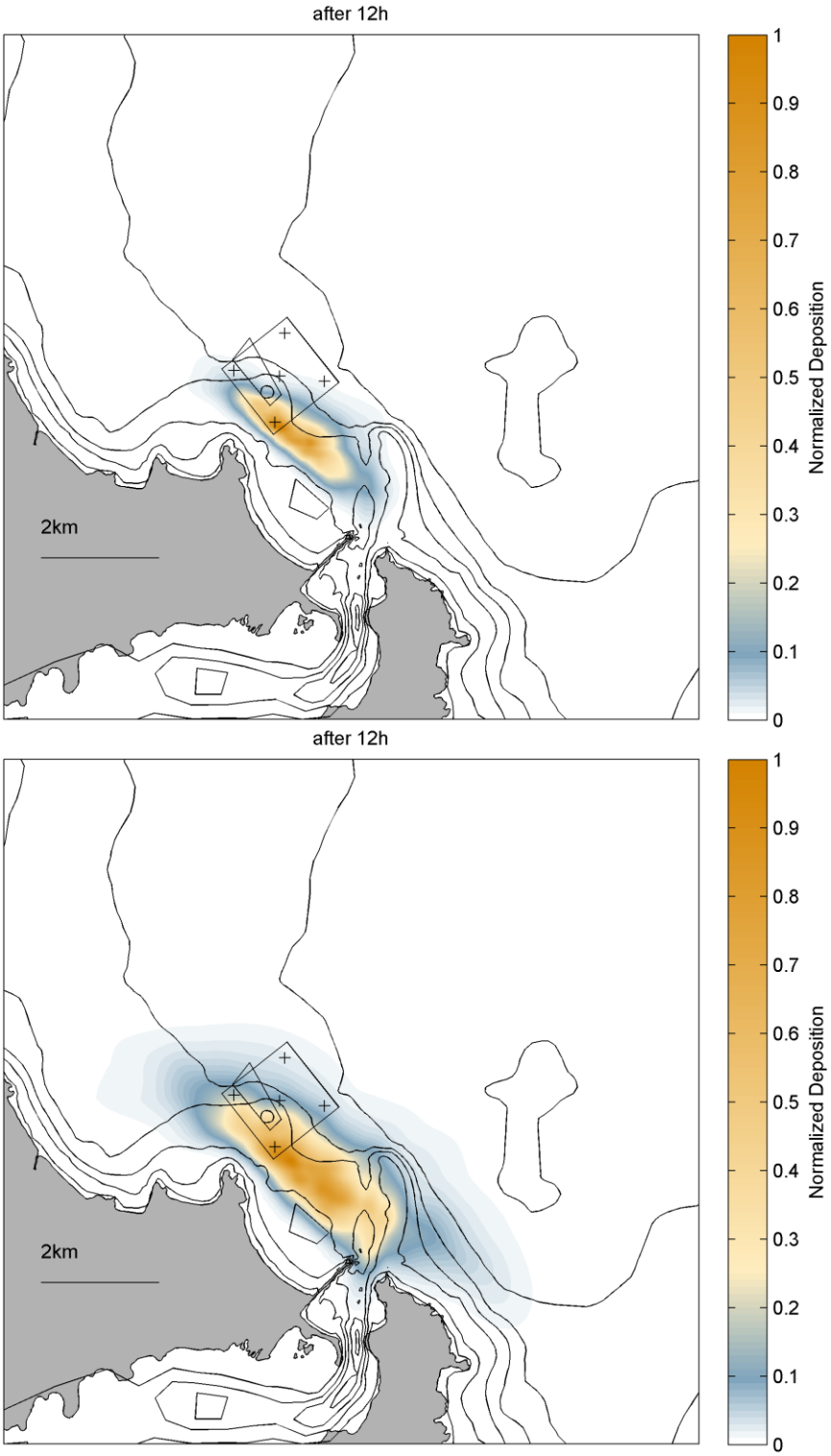

Figure 3.14 Normalized deposition for a release of silt at site 3 (top: New Era, bottom: TSHD).

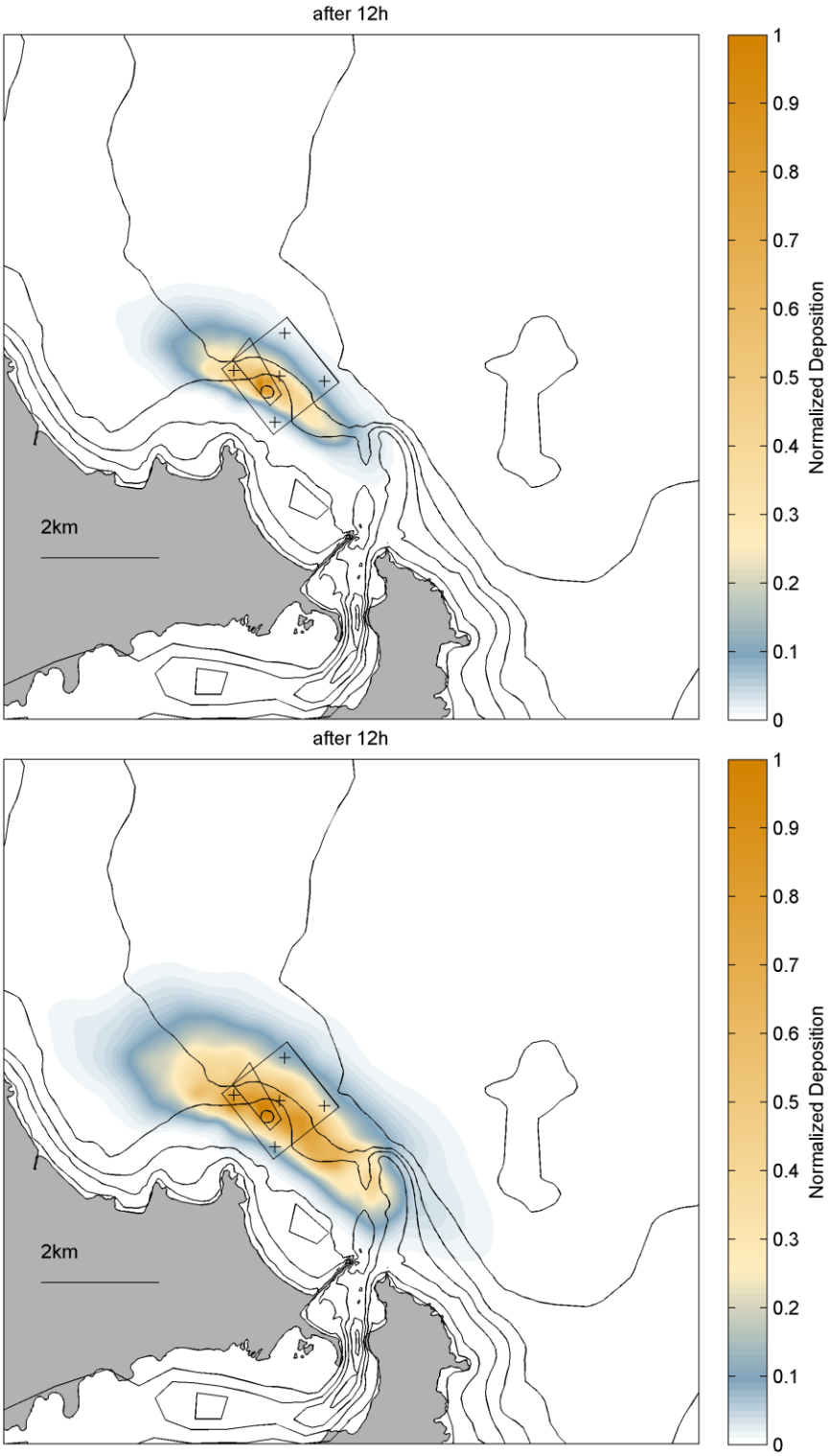

Figure 3.15 Normalized deposition for a release of silt at site 4 (top: New Era, bottom: TSHD).

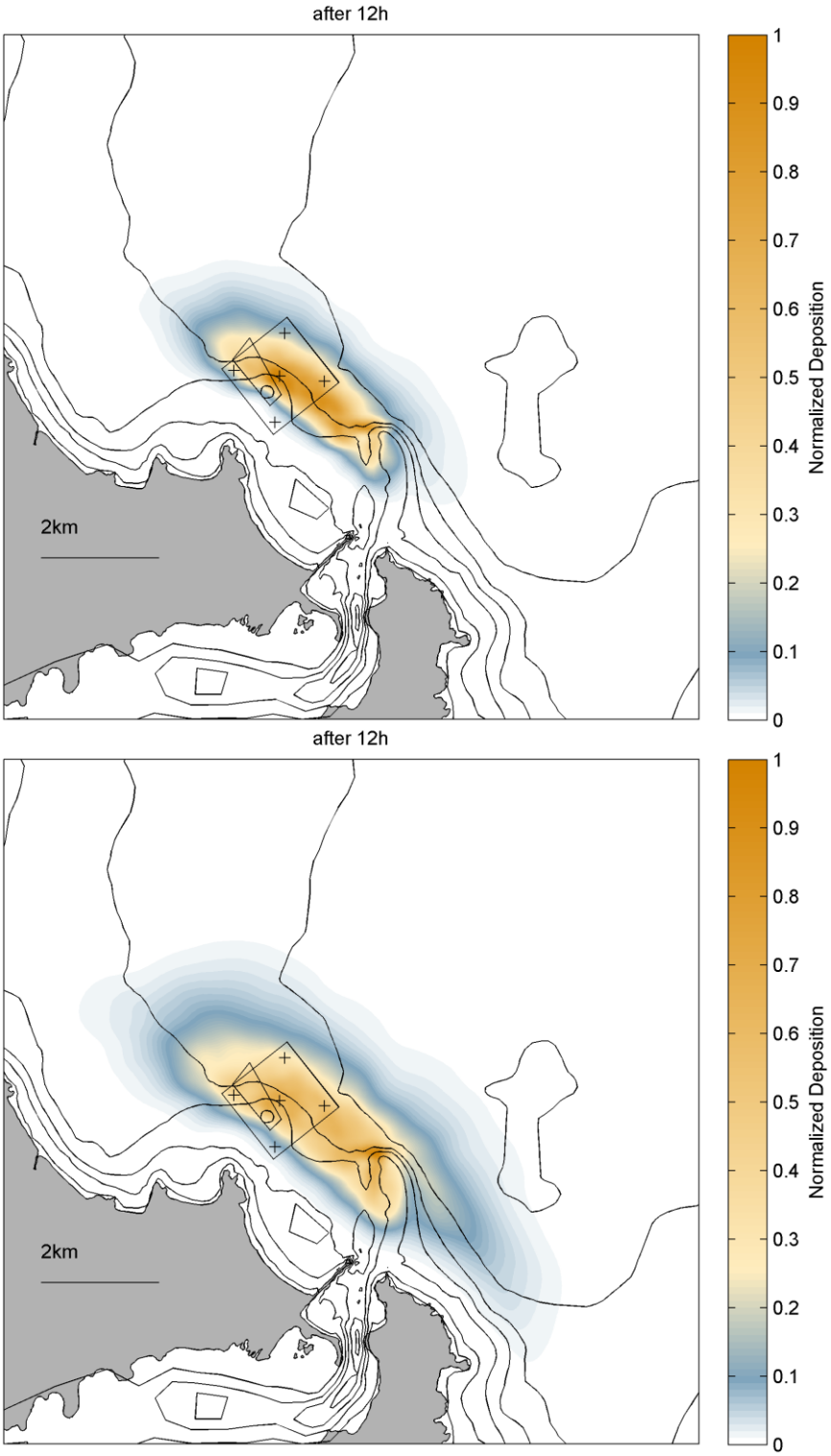

Figure 3.16 Normalized deposition for a release of silt at site 5 (top: New Era, bottom: TSHD).

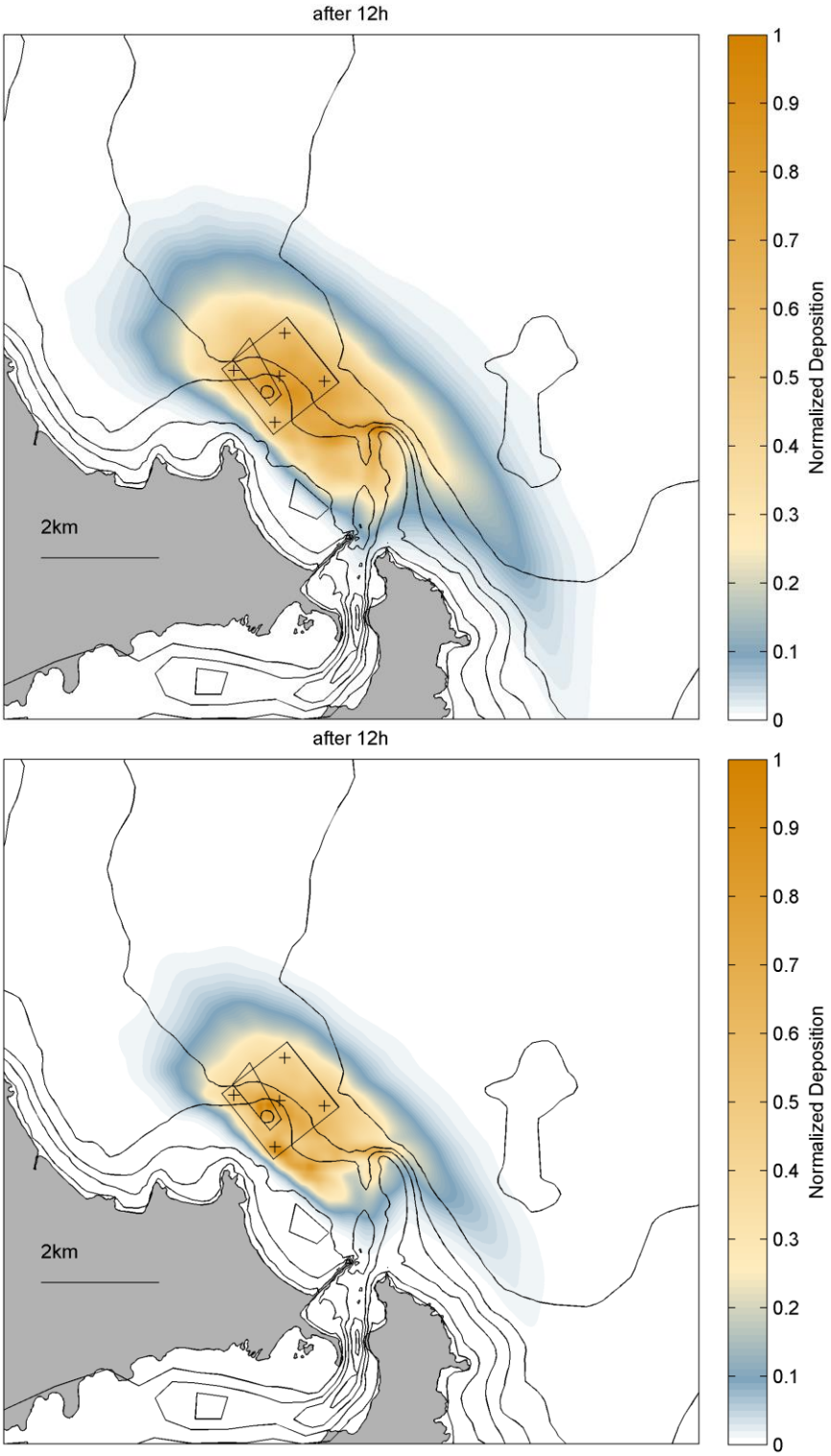

Figure 3.17 Normalized deposition for releases of silt at all sites (top: New Era, bottom: TSHD).

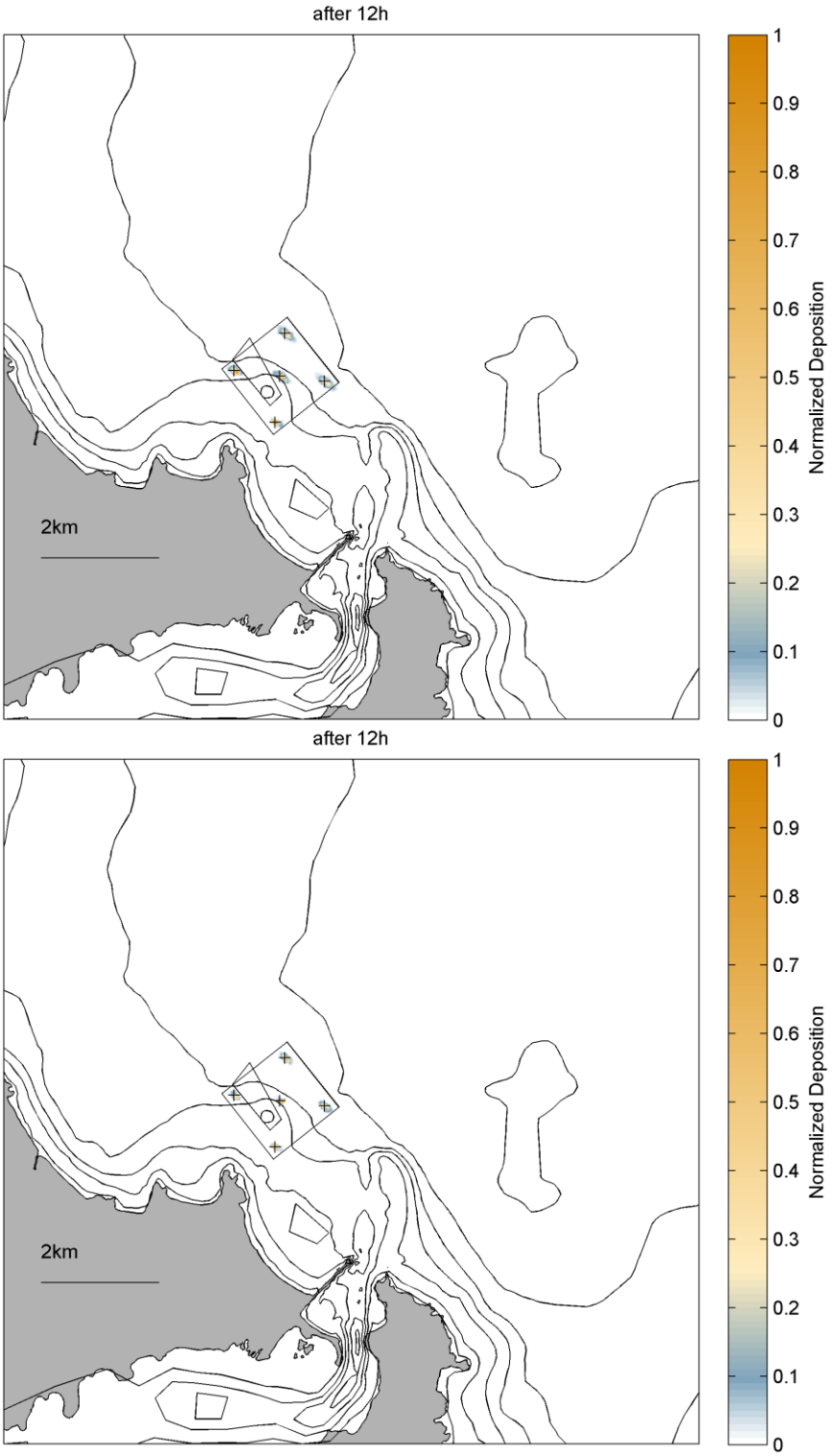

Figure 3.18 Normalized deposition for releases of fine sand at all sites (top: New Era, bottom: TSHD).

3.4. Probabilistic excursion footprints

Probabilistic excursion footprints provide information on the general region of influence of the simulated particle cloud which represents the passive plume. Here, footprint contours including 90, 95 and 99 % of the settled particles are presented in Figure 3.19 to Figure 3.24 for the five release sites considered.

Using the center of the disposal site as reference point, the 90 and 99th percentiles contours for the New Era case respectively extend ~3.0 to 4.0 km to the northwest, 3.5 to 4.5 km to the east-northeast and up to ~6.5 - 8.0 km to the southeast. For the TSHD case, the 90 and 99th percentiles contours respectively extend ~2.5 to 3.5 km to the northwest, 3.0 to 4.0 km to the east-northeast and up to ~5.0 - 7.0 km to the southeast.

Summary percentiles contours combining results for all release sites are included in Figure 3.25 and Figure 3.26 for silt and fine sand respectively (i.e. largest and smallest dispersions expected).

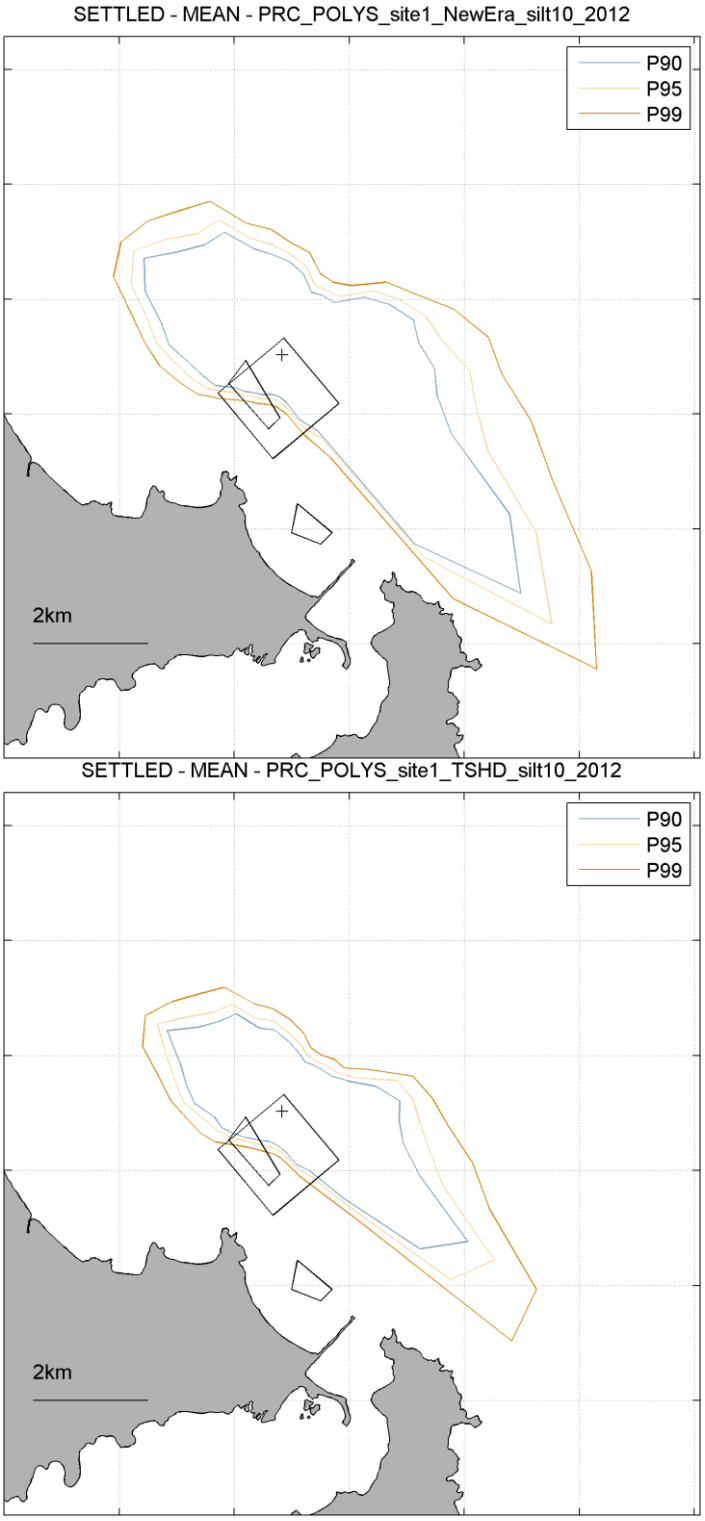

Figure 3.19 Mean excursion contours of deposited particles for the 90th, 95th and 99th percentile levels for a release of silt at site 1 (top: New Era, bottom: TSHD).

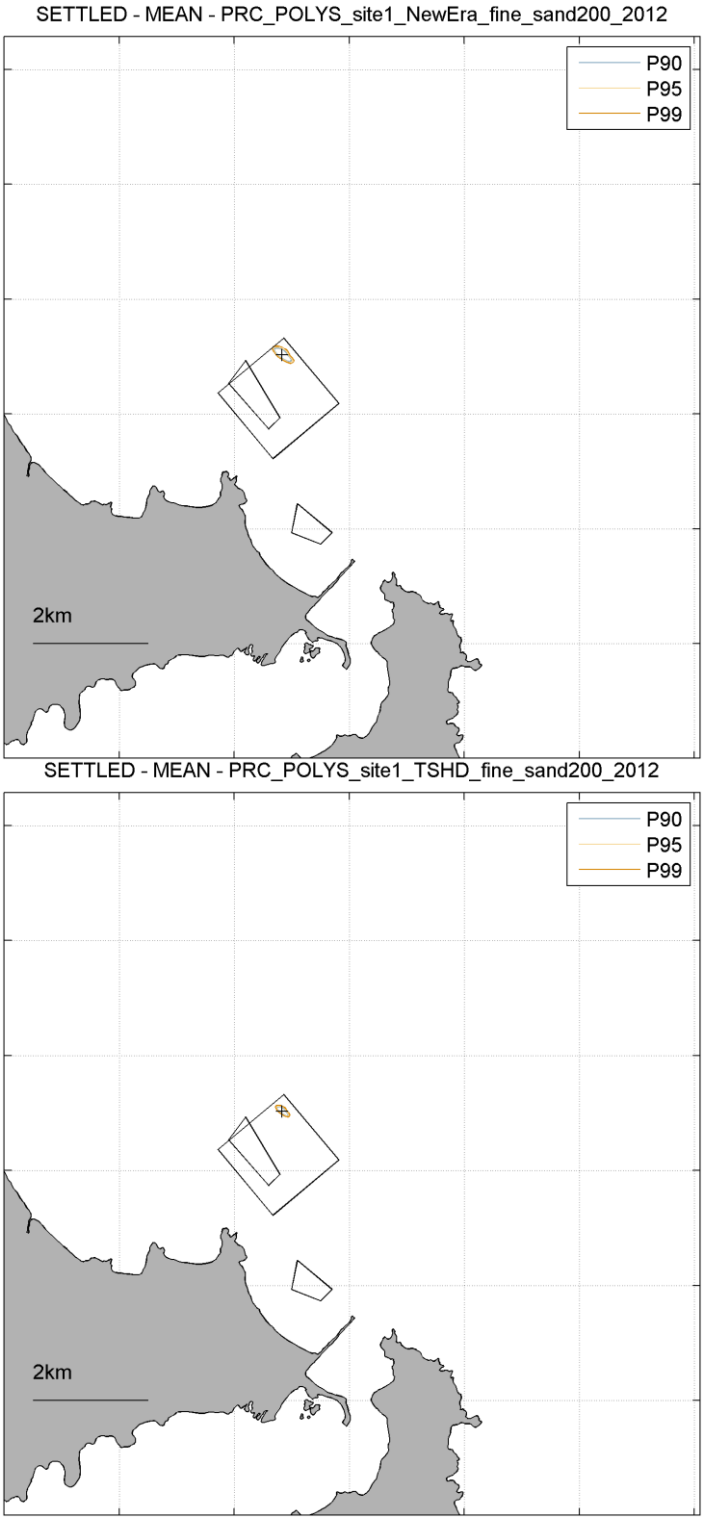

Figure 3.20 Mean excursion contours of deposited particles for the 90th, 95th and 99th percentile levels for a release of fine-sand at site 1 (top: New Era, bottom: TSHD).

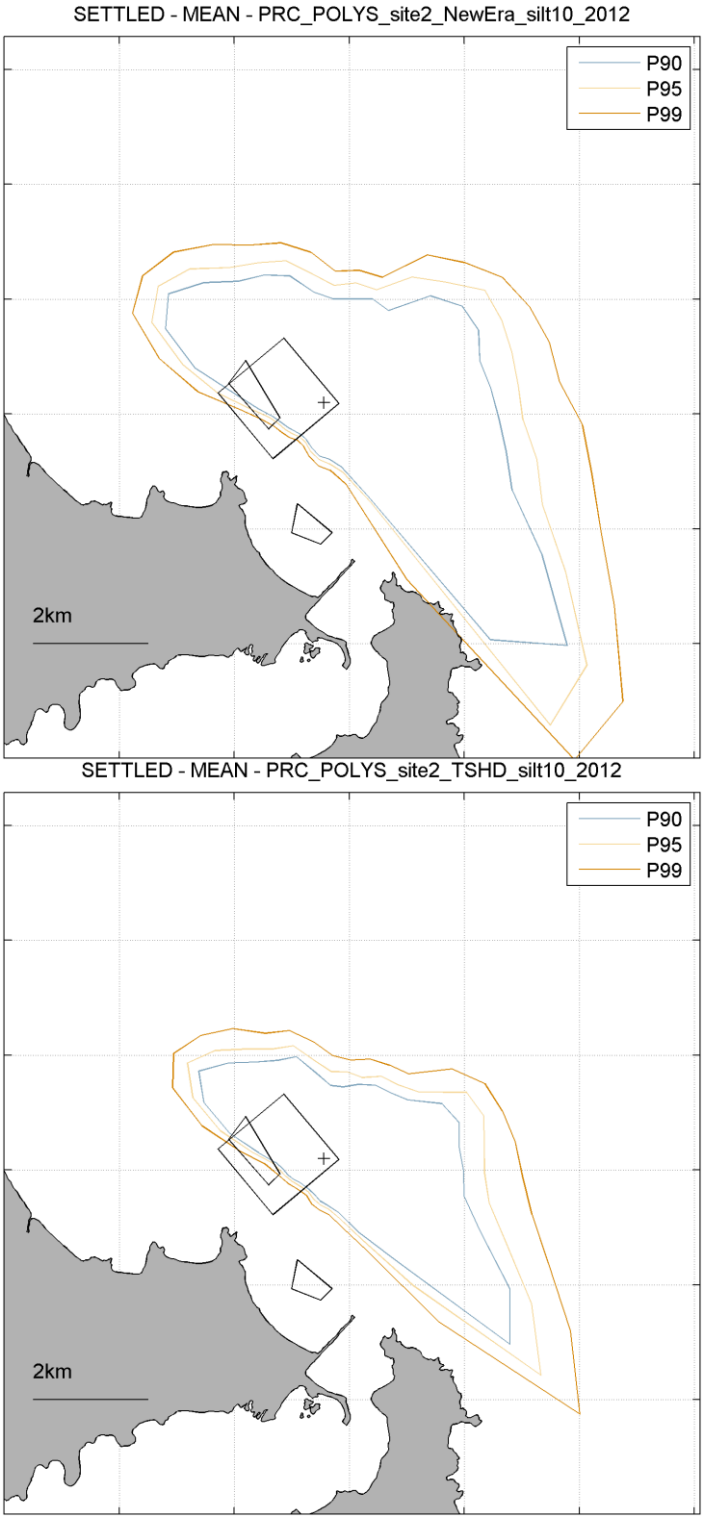

Figure 3.21 Mean excursion contours of deposited particles for the 90th, 95th and 99th percentile levels for a release of silt at site 2 (top: New Era, bottom: TSHD).

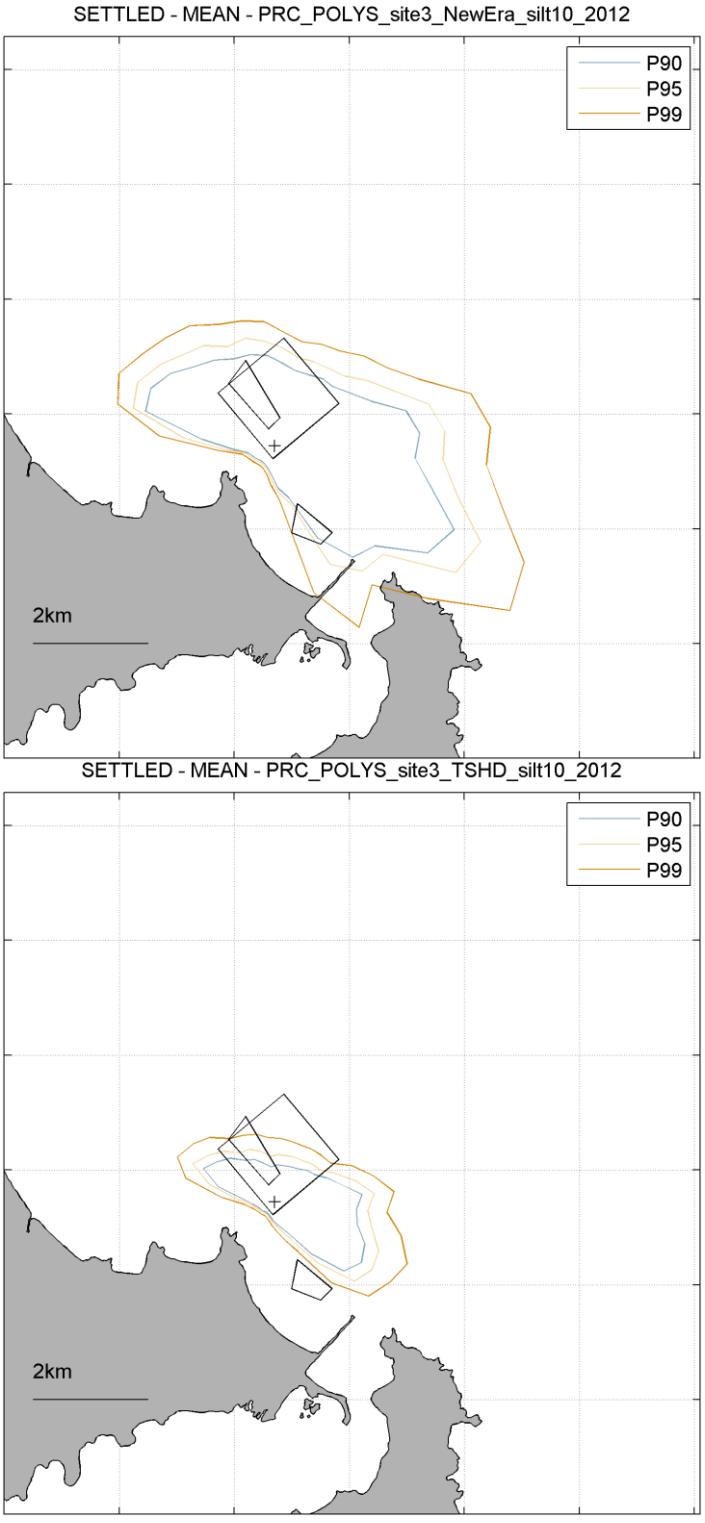

Figure 3.22 Mean excursion contours of deposited particles for the 90th, 95th and 99th percentile levels for a release of silt at site 3 (top: New Era, bottom: TSHD).

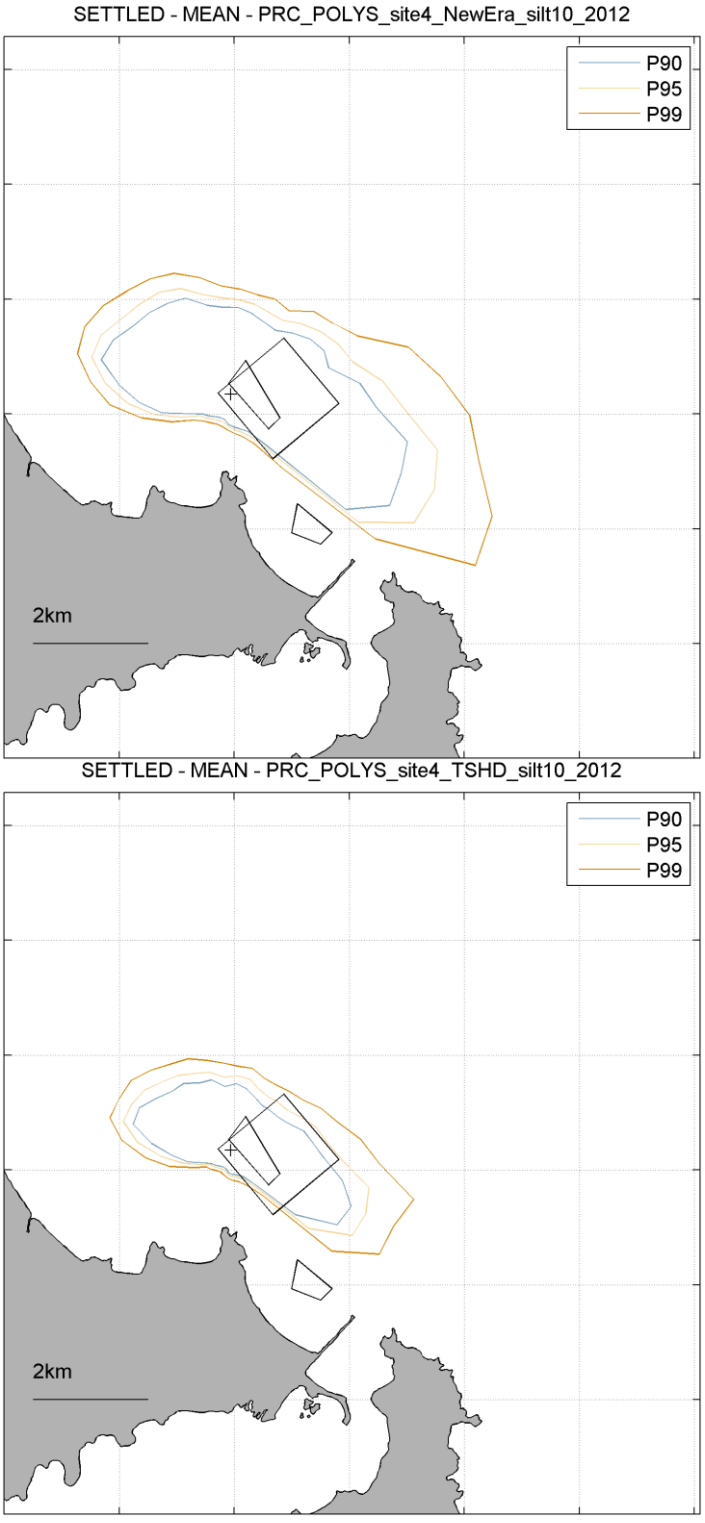

Figure 3.23 Mean excursion contours of deposited particles for the 90th, 95th and 99th percentile levels for a release of silt at site 4 (top: New Era, bottom: TSHD).

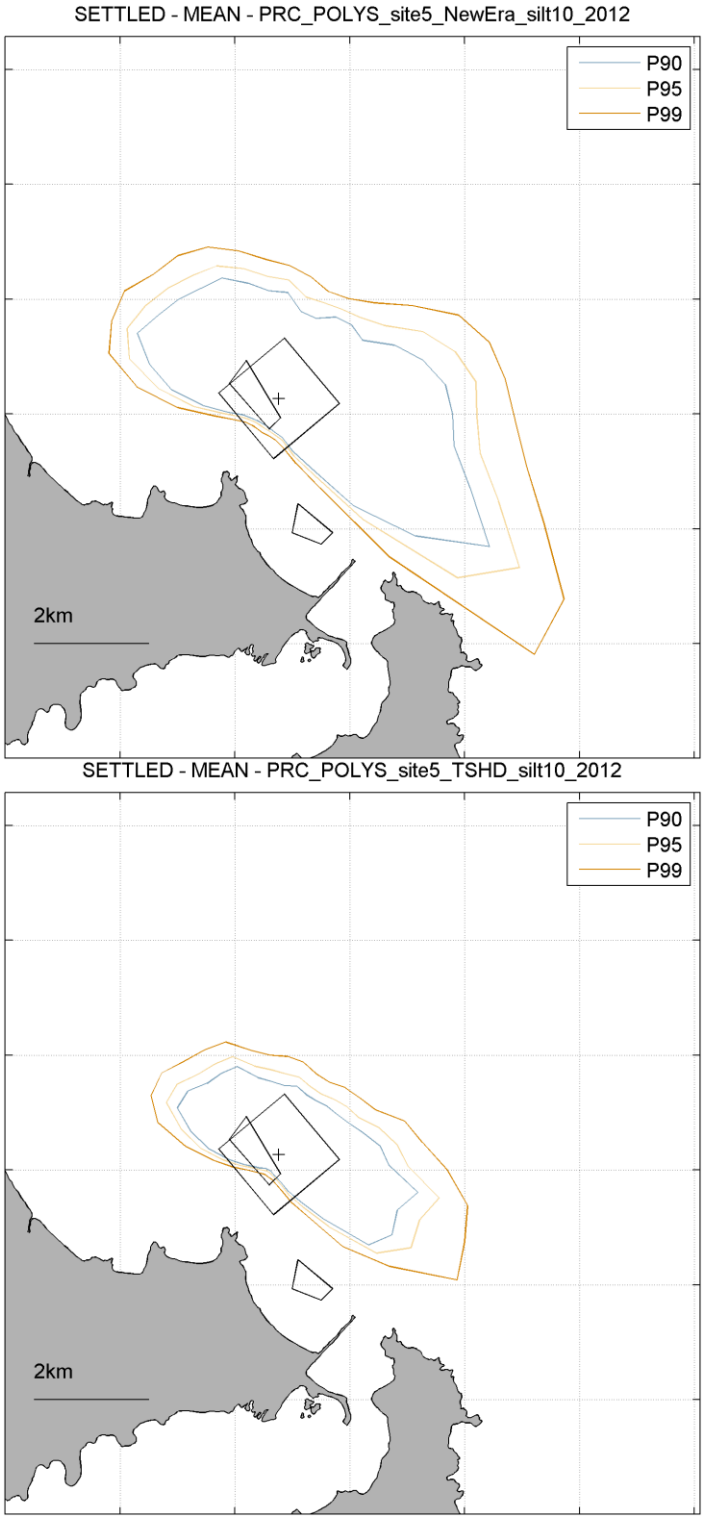

Figure 3.24 Mean excursion contours of deposited particles for the 90th, 95th and 99th percentile levels for a release of silt at site 5 (top: New Era, bottom: TSHD).

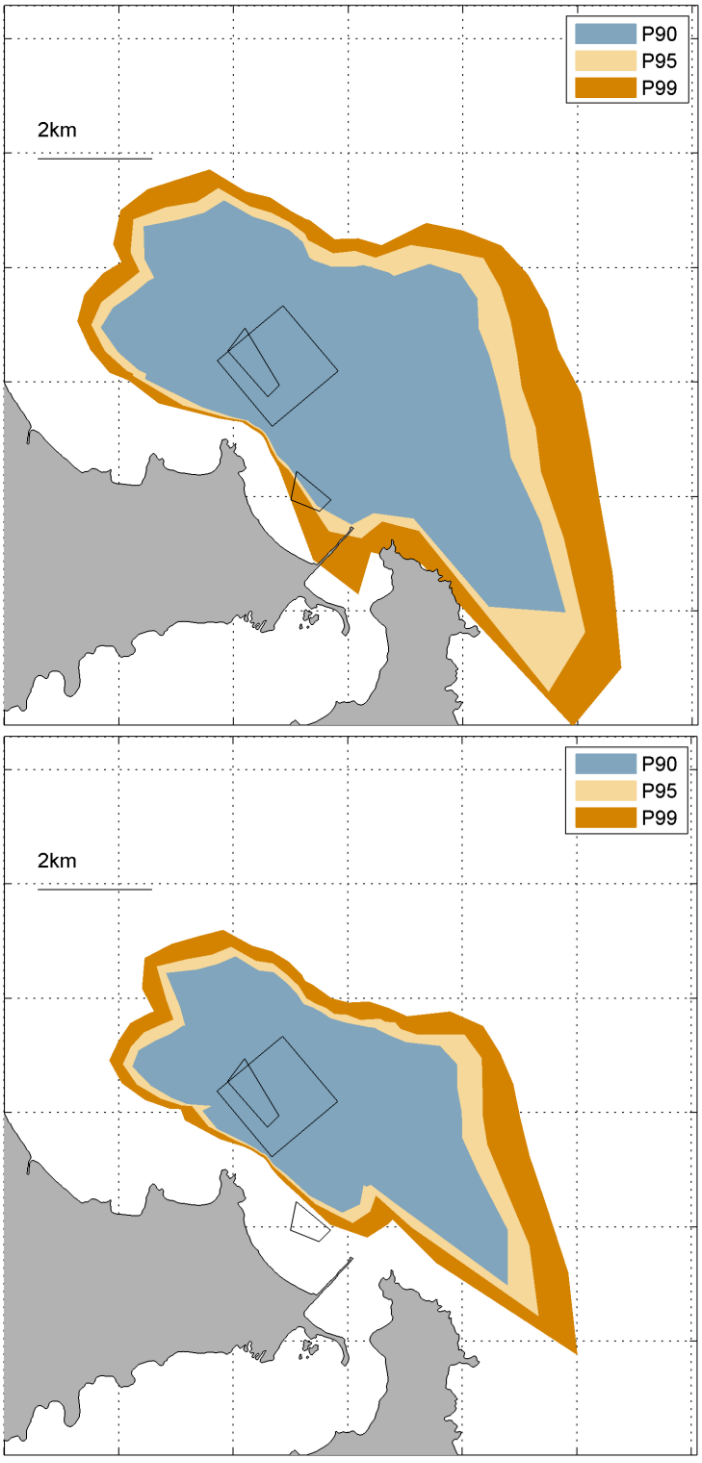

Figure 3.25 Combined mean excursion contours of deposited particles for the 90th, 95th and 99th percentile levels for releases of silt at all sites (top: New Era, bottom: TSHD).

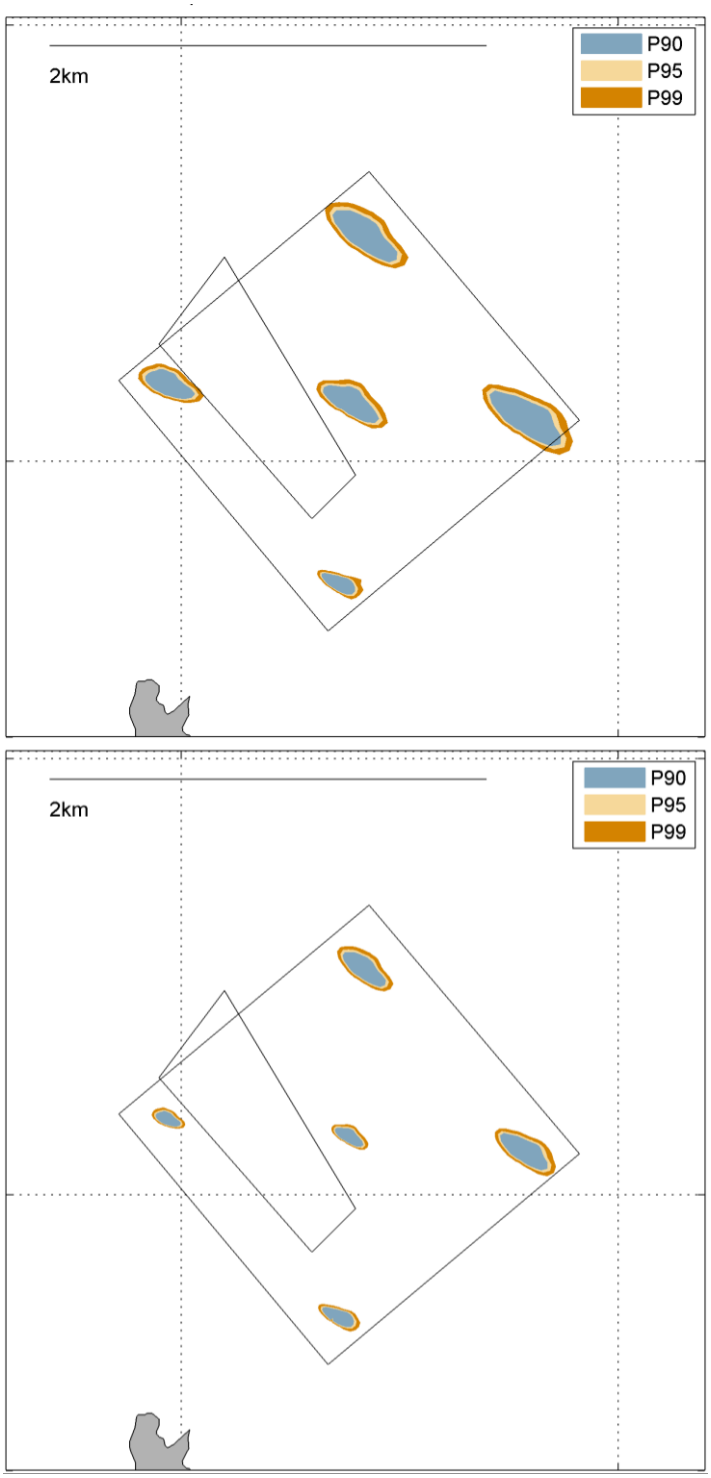

Figure 3.26 Combined mean excursion contours of deposited particles for the 90th, 95th and 99th percentile levels for releases of fine sand at all sites (top: New Era, bottom: TSHD).

4. CONCLUSIONS

Particle-tracking simulations were undertaken to assess the dispersion and settling characteristics of the passive plume resulting from sediment disposal at the proposed new Heyward Point Disposal Ground. Two representative sediment classes were considered in the simulations namely fine sand and silt. Five different release sites throughout the ground were simulated to capture the variability of the ambient hydrodynamic forcing and two release depths relating to different dredge vessels to be used were included. Since the timing and duration of the disposal activities are unknown, simulations were run over a year long period and results were averaged to provide a robust probabilistic picture of the passive plume dispersion and settling features.

The hydrodynamic regime throughout the ground is essentially bi-modal with either northwest or southeast-directed flows. Southeast-directed flows are more frequent and stronger. Mean flow velocities at release sites are southeast-directed of order 0.1 m/s. Maximum velocities are of ~0.5 m/s.

The ambient hydrodynamic forcing results in SSC and deposition footprints that are elongated in the northwest-southeast axis, with larger extents in the southeast direction. Deposition footprints typically extend ~2-4 km southeast from the release sites (i.e. reaching Tairoa Heads and possibly further) and 1-2 km towards the northwest. Deposition patterns consistently cross the Harbour entrance region with some sedimentation predicted within the outer entrance channel.

5. REFERENCES

Aarninkhof, S., Luijendijk, A., 2009. Safe disposal of dredged material in an environmentally sensitive environment. Terre et Aqua 119, 21-28

Berlamont J, Ockenden M, Toorman E, Winterwerp J (1993). The characterisation of cohesive sediment properties. Coastal Engineering 21, 105–128.

Bokuniewicz, H. J., Gebert,J, Gordon, R.B., Higgins, J.L., Kaminsky, P. (1978). Field Study of the Mechanics of the Placement of Dredged Material at Open-Water Sites. Prepared by Yale University for the US Army Engineer Waterways Experiment. Technical Report D-78-79

Egbert, G. and Erofeeva, L. (2002) Efficient inverse modelling of barotropic ocean tides. *Journal of Atmospheric and Oceanic Technology*, 19, N2

Flather, R.A. (1976) A tidal model of the northwest European continental shelf. *Memoires de la Societe Royale des Sciences de Liege* 6 (10), 141-164

HR Wallingford, 2010. TASS Software - Trailer suction hopper dredger, User guide for TASS version 3.2.1. Report prepared by HR Wallingford for the EcoShape Project (No. Rev. 7).

Marchesiello, P., McWilliams, J.C. and A. Shchepetkin (2001) Open boundary conditions for long-term integration of regional oceanic models. Ocean Modelling, 3, 1-20.

Mellor, G.L. (2004) Users guide for "A three-dimensional, primitive equation, numerical ocean model". Princeton University, Princeton, NJ. Available from: http://www.aos.princeton.edu/WWPUBLIC/htdocs.pom/

Metocean Solutions Limited., to be released. Port Otago wave and sediment dynamics study - Setup and validation of numerical models of waves, hydrodynamics and sediment transport.

Okubo, A., 1971. Oceanic diffusion diagrams. Deep-Sea Research 18, 789-802.

Orlanski, I. (1976) A simple boundary condition for unbounded hyperbolic flows. *Journal of Computational Physics* 21, 251-269.

Saha, S., Moorthi, S., Pan, H.-L., Wu, X., Wang, J., Nadiga, S., Tripp, P., Kistler, R., Woollen, J., Behringer, D., Liu, H., Stokes, D., Grumbine, R., Gayno, G., Wang, J., Hou, Y.-T., Chuang, H.-Y., Juang, H.-M.H., Sela, J., Iredell, M., Treadon, R., Kleist, D., Van Delst, P., Keyser, D., Derber, J., Ek, M., Meng, J., Wei, H., Yang, R., Lord, S., Van Den Dool, H., Kumar, A., Wang, W., Long, C., Chelliah, M., Xue, Y., Huang, B., Schemm, J.-K., Ebisuzaki, W., Lin, R., Xie, P., Chen, M., Zhou, S., Higgins, W., Zou, C.-Z., Liu, Q., Chen, Y., Han, Y., Cucurull, L., Reynolds, R.W., Rutledge, G., Goldberg, M., 2010. The NCEP Climate Forecast System Reanalysis. Bulletin of the. American. Meteorology. Society. 91, 1015–1057. doi:10.1175/2010BAMS3001.1.

Smith, S. J. and C. T. Friedrichs, 2011. Size and settling velocities of cohesive flocs and suspended sediment aggregates in a trailing suction hopper dredge plume. Continental Shelf Research 31(10, Supplement),S50 – S63

Spearman, J., Bray, R.N., Land, J., Burt, T.N., Mead, C.T., Scott, D., 2007. Plume dispersion modelling using dynamic representation of trailer dredger source terms. In: Estuarine and Coastal Fine Sediments Dynamics. Eds: Maa, J.P.Y., Sanford, L.P. and Schoellhamer, D.H. Elsevier 2007, 417-448.

Spearman, J., De Heer, A. and Aarninkhof , S.G.J. and Van Koningsveld, M. 2011. Validation of The TASS System For Predicting The Environmental Effects Of Trailing Suction Hopper Dredging,Terra et Aqua, 125, p14.

USACE-EPA, 1998. Evaluation of Dredged Material Proposed For Discharge in Waters of the U.S. - Testing Manual. Prepared by Enviroment Protection Agency and and United States Army Corps of Engineers, Washington, D.C. 87. pp

Van Rijn, L.C., 1993. Principles of Sediment Transport in Rivers, Estuaries, Coastal Seas and Oceans (in Press). Aqua Publications, P.O. Box 9896, Amsterdam, The Netherlands.

Vitali L., Monforti F., Bellasio R., Bianconi R., Sachero V., Mosca S. and Zanini G., 2006. Validation of a Lagrangian dispersion model implementing different kernel methods for density reconstruction. Atmospheric Environment 40, 8020-8033.

Zhang, Y. L. and Baptista, A.M., 2008. SELFE: A semi-implicit Eulerian-Lagrangian finite-element model for cross-scale ocean circulation. Ocean Modelling, 21 (3-4), 71-96.